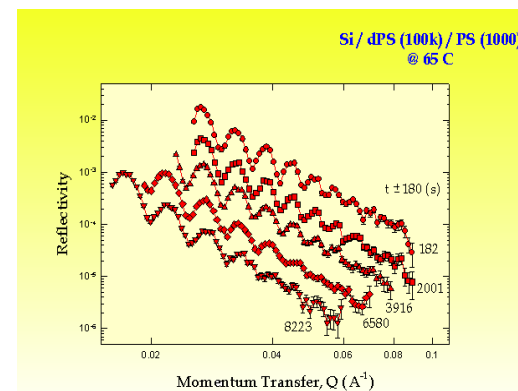
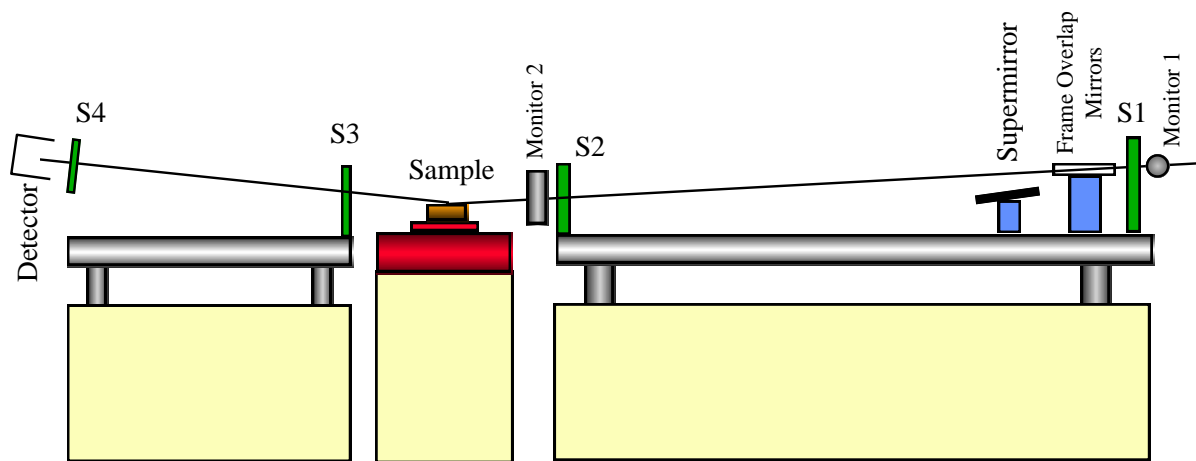


Introduction to Neutron Reflectivity

J.R.P. Webster

ISIS Facility, Rutherford Appleton Laboratory

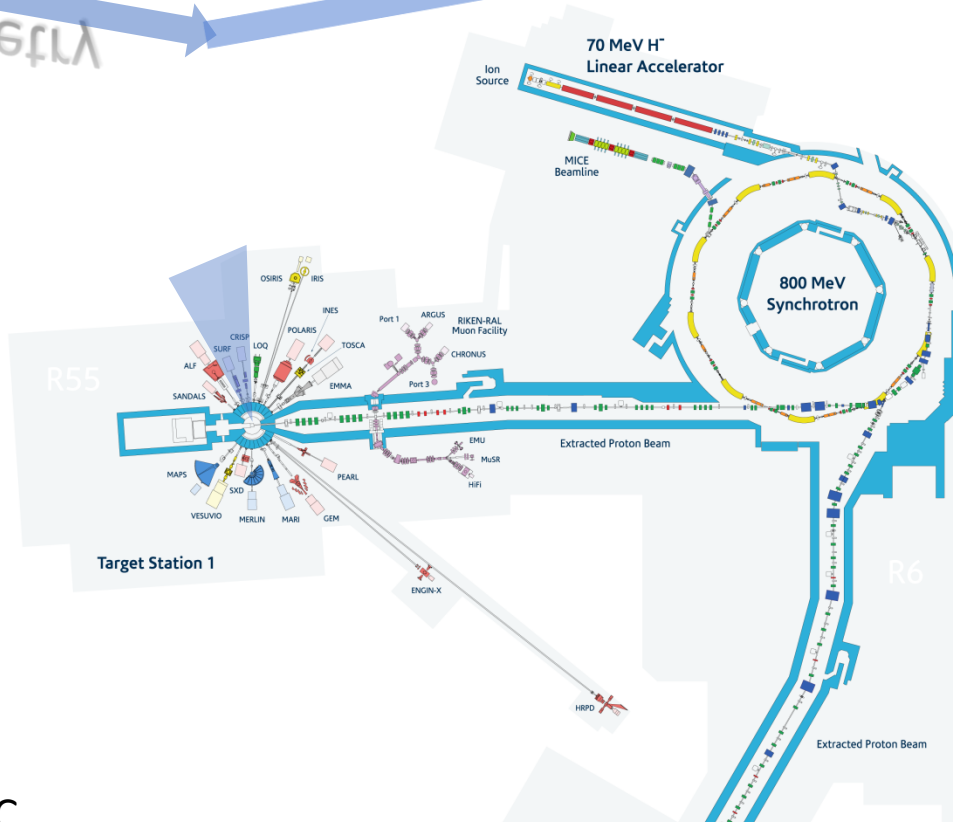


Reflectometry

REFLECTOMETRY

TS1

CRISP
SURF



TS2

OFFSPEC
INTER
POLREF

Types of Instrument at ISIS

- Diffractometer
- Reflectometer
- Small Angle Scattering
- Indirect Spectrometer
- Direct Spectrometer
- Muon Spectrometer/Instrument
- Chip Irradiation
- Imaging and Diffraction

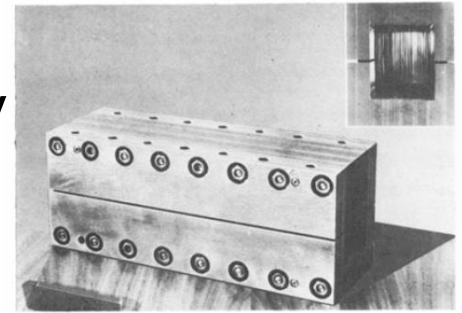


Neutrons – a tailor-made probe

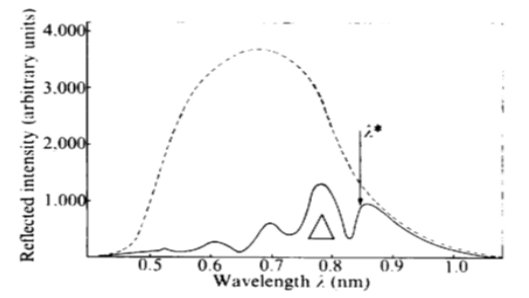
- **Neutron wavelength and energy ‘just right’ for condensed matter** - *structure and dynamics*
- **Neutron cross-section** - *isotopic dependence*
- **H / D contrast** - *nuclear form factor*
- **Magnetic Moment** - *magnetic order*
- **Weak probe** - *theoretical interpretation*
- **Highly penetrating** - *bulk probe - complex SE*
- **Non Destructive**

Evolution of Neutron Reflectivity (ISIS centric)

- 1965 Koester: gravity mirror
determination of scattering lengths
- 1976 Hayter, Penfold, Williams
first interference fringes
- 1981 Application of NR to chemical
surfaces and interfaces
(Faraday Trans, D17)
- 1986 Argonne IPNS polarised
reflectometer (Gian Felcher)
CRISP 1st spectrum (august)
- 1988 Spread monolayers (Richardson)
- 1998 Adsorption at the Liquid Surface
(Penfold, Thomas)



Polarising Soller Guide



Fe/Co thin film: Nature, 262, 1976, 569

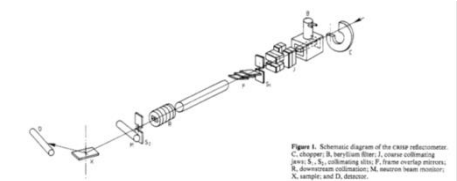
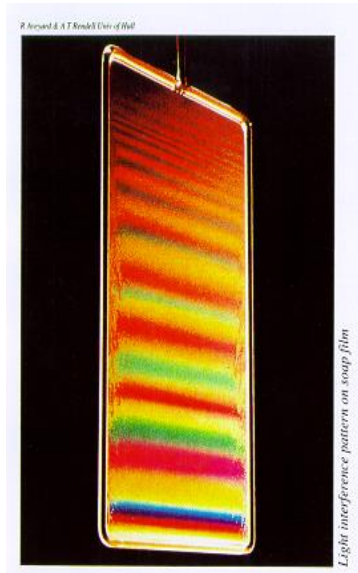
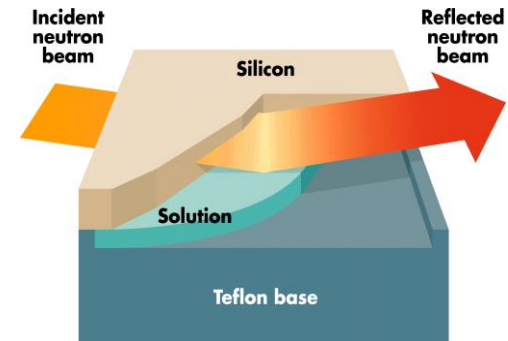


Figure 1. Schematic diagram of the chopper reflectometer:
 C, Chopper; M, monochromator; P, polarizing filter;
 S, sample; D, detector; A, B, C, D, E, F, frame overlap mirrors;
 G, detector collimator; H, neutron beam monitor;
 X, sample; and D, detector.

Specular reflection of neutrons from surfaces and interfaces

Analogous to optical interference,
ellipsometry

Equivalent to electromagnetic radiation with
electric vector perpendicular to the plane
of incidence



Depth Profiling : provides
information on concentration
or composition profile perpendicular
to the surface or interface

(Penfold, Thomas, *J Phys Condens Matt*, 2
(1990)1369,
T P Russell, *Mat Sci Rep* 5 (1990) 171)

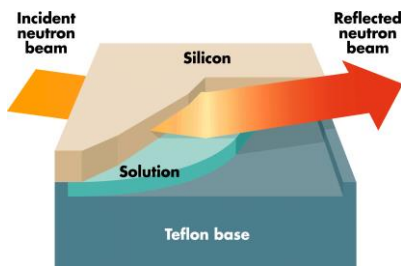
Reflectometry

Kinetics

- Polymer Diffusion
- Critical exponents in SCF
- Protein unfolding
- Non equilibrium surfactant films
- Temporal resolution of
 - Ion transfers
 - Solvent transfers
 - Polymer structure

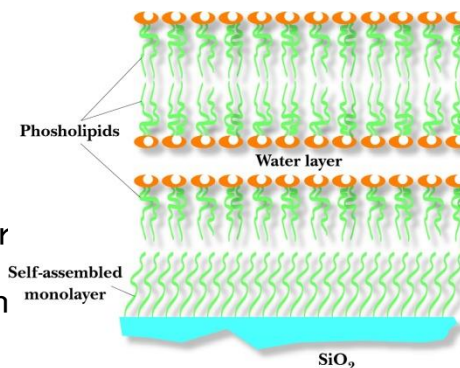
Electrochemistry

- Electrodeposition and Surface nucleation
- Self Assembly of systems
 - Metal Hydroxide electroprecipitation (batter
 - Novel templating mechan



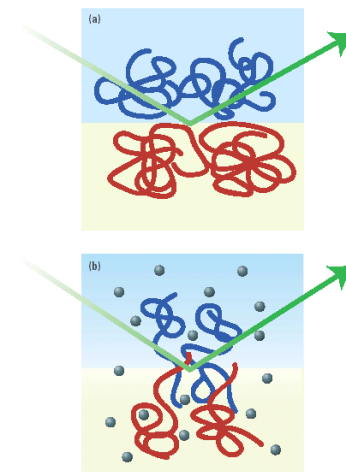
Surfactants

- Parametric Studies
- Liquid/Liquid Interface
- Reduce Label size in Structural Studies
- Self Assembly
- Foams



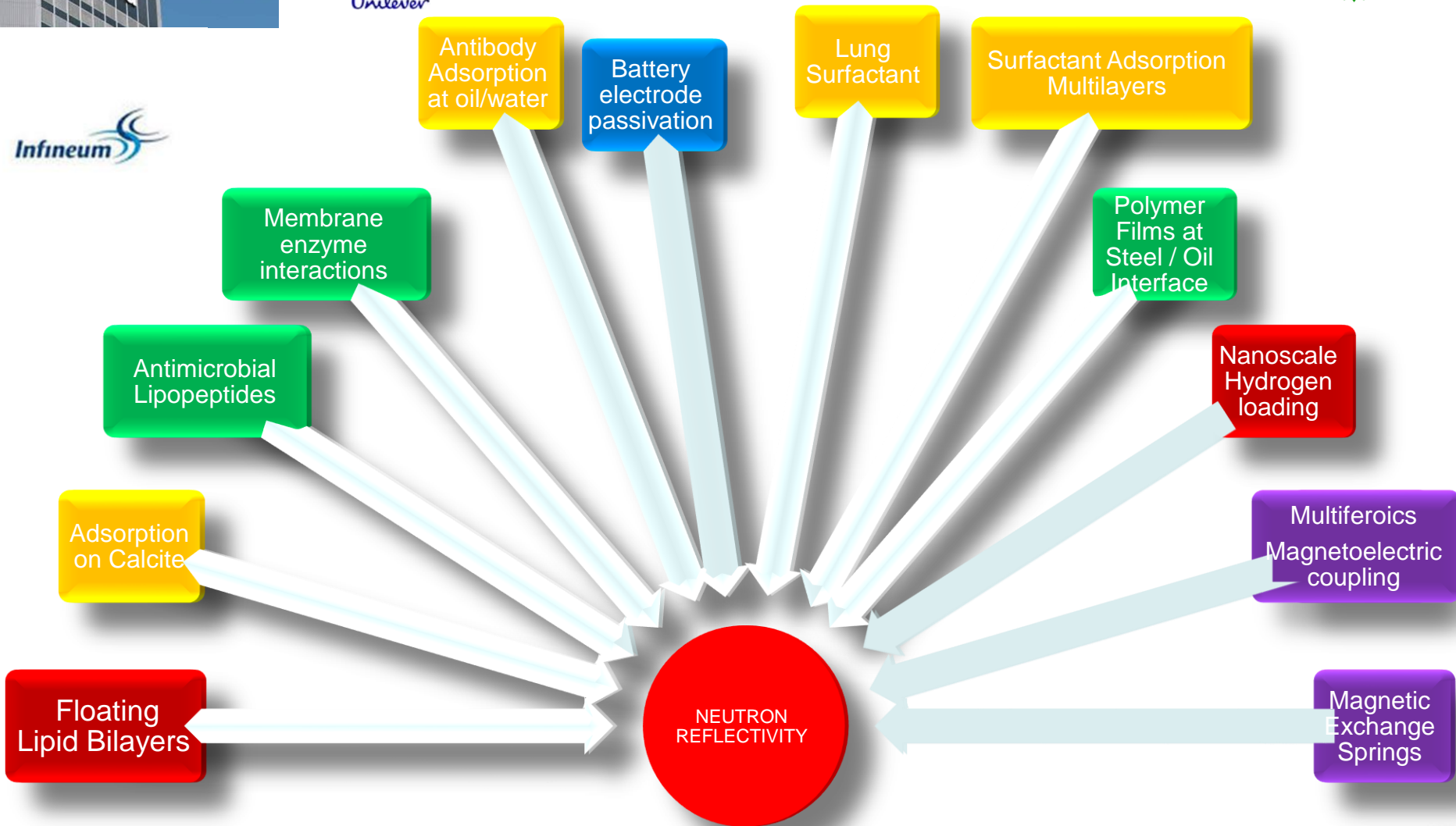
Model Devices

- Thin polymer films (finite size effects)
- Spin coating



Biology

- Protein adsorption
- Biocompatible polymers
- Drug transport
- Anaesthesia mechanisms



Unipath Ltd



CRODA

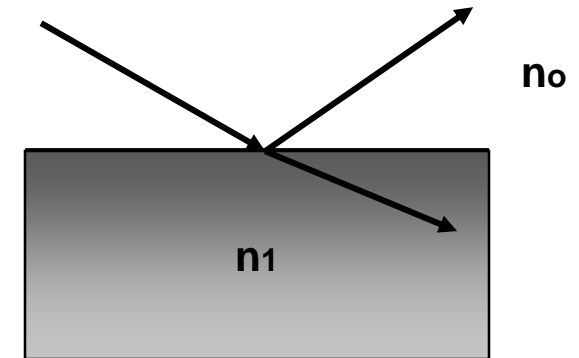


Science & Technology Facilities Council
ISIS Neutron and Muon Source

Specular reflection of neutrons

Refractive index defined using the usual convention in optics:

$$n = k_1 / k_0$$



$$n = 1 - \lambda^2 A - i\lambda B$$

$$A = Nb / 2\pi$$

$$B = N(\sigma_a + \sigma_i) / 4\pi$$

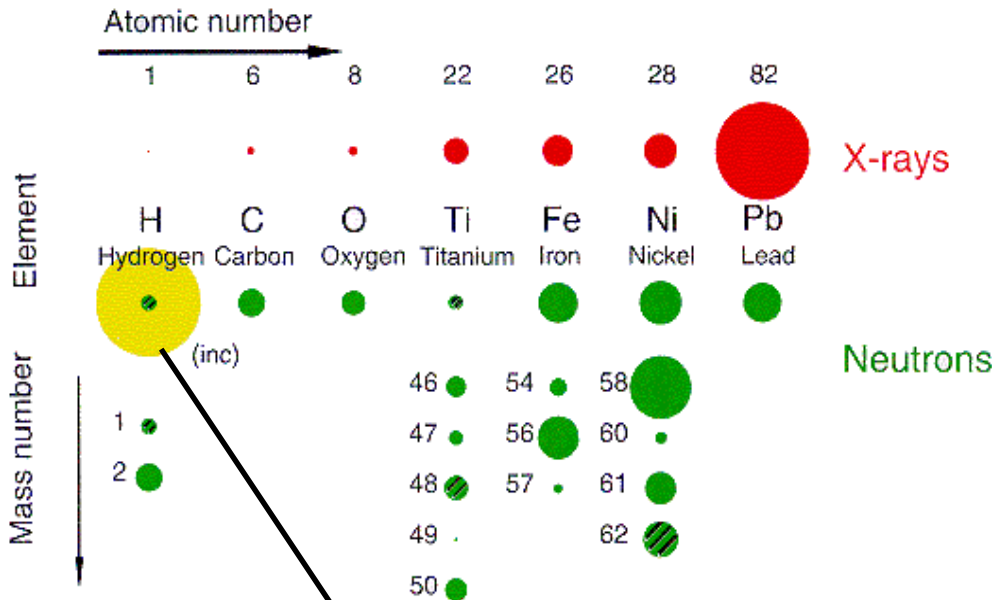
X-rays

$$n = 1 - \alpha - i\beta$$

$$\alpha = N\lambda^2 Z_{re} / 2\pi$$

$$\beta = \lambda \mu / 4\pi$$

Refractive Index for neutrons



The diameters of the circles shown scale with the scattering amplitude f_1 ($\sin\theta=0$) for x-rays, and $b_{coh} \times 10$ for neutrons. Hatching indicates negative scattering amplitudes.

$$n = \frac{k_1}{k_0}$$

$$n = 1 - \lambda^2 A - i\lambda B$$

$$A = Nb/2\pi$$

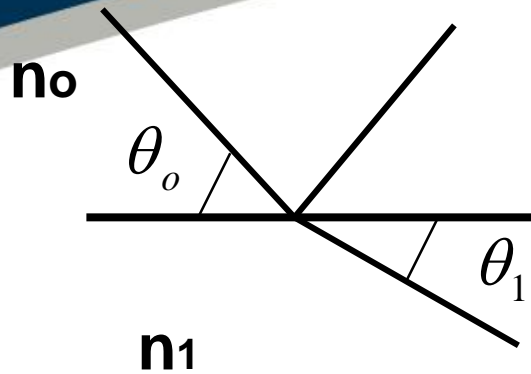
Extensively use H/D isotopic substitution to manipulate "contrast" or refractive index

H -0.374×10^{-12} cm

D 0.667×10^{-12} cm

$n < 1.0$ hence **TOTAL EXTERNAL REFLECTION**

Specular reflection of neutrons (some basic optics)

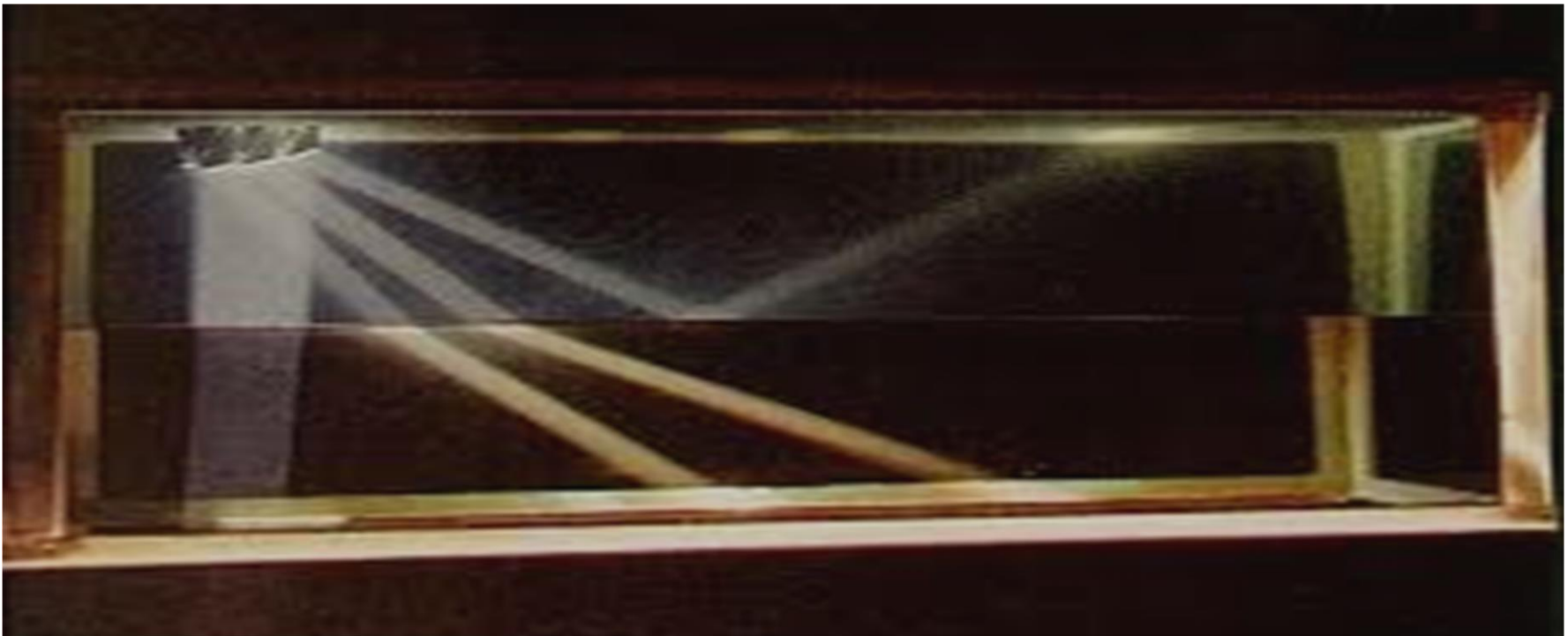


From Snell's Law,
$$n = \frac{n_1}{n_0} = \frac{\cos \theta_0}{\cos \theta_1}$$

At total reflection $\theta_0 = \theta_c$
 $\theta_1 = 0.0$ $\cos \theta_1 = 1.0$

Critical angle

Total reflection ($R=1.0$) for $\theta < \theta_c$



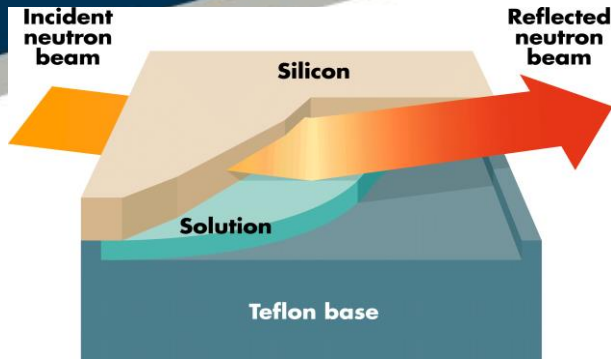


Some typical values for θ_c and σ_a

Material	θ_c (deg / Å)
Ni	0.1
Si	0.047
Cu	0.083
Al	0.047
D ₂ O	0.082

Material	σ_a (barns)
Si	0.17
Cu	3.78
Co	37.2
Cd	2520
Gd	29400
Al	0.231

Specular Neutron Reflection (simple interface)

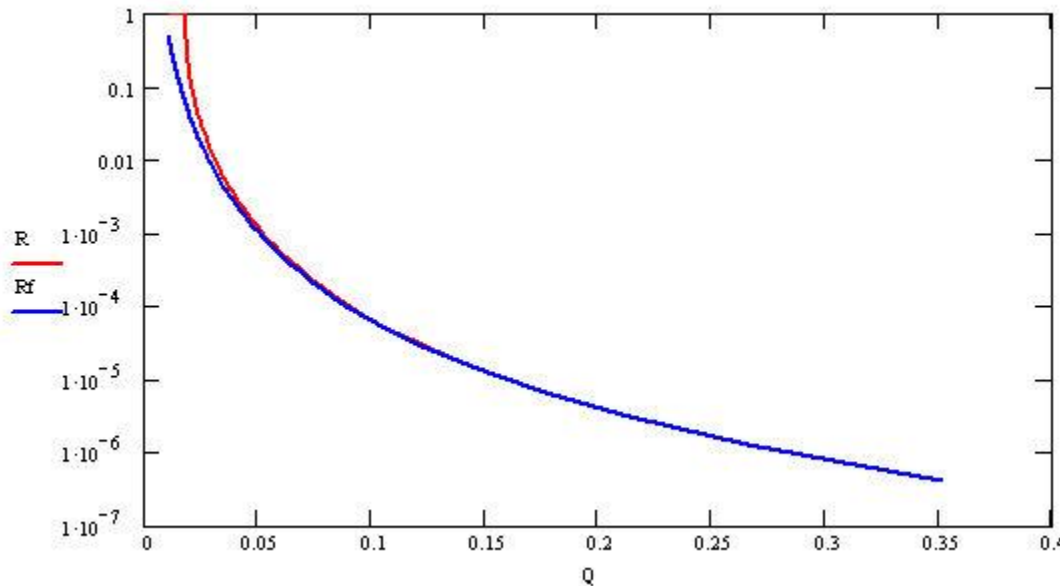


Within **Born Approximation** the Reflectivity is given as,

$$R(Q) = \frac{16\pi^2}{Q^4} \left| \int \rho(z) e^{-iQz} dz \right|^2$$

$$Q = k_1 - k_2 = 4\pi \sin \theta / \lambda$$

Reflectivity from a simple single interface is then given by **Fresnel's Law**



$$= \left| \frac{n_0 \sin \theta_0 - n_1 \sin \theta_1}{n_0 \sin \theta_0 + n_1 \sin \theta_1} \right|^2$$

$$r(Q) = \frac{16\pi^2}{Q^4} \Delta\rho^2$$

Specular Neutron Reflection

For thin films see interference effects that can be described using standard thin film optical methods

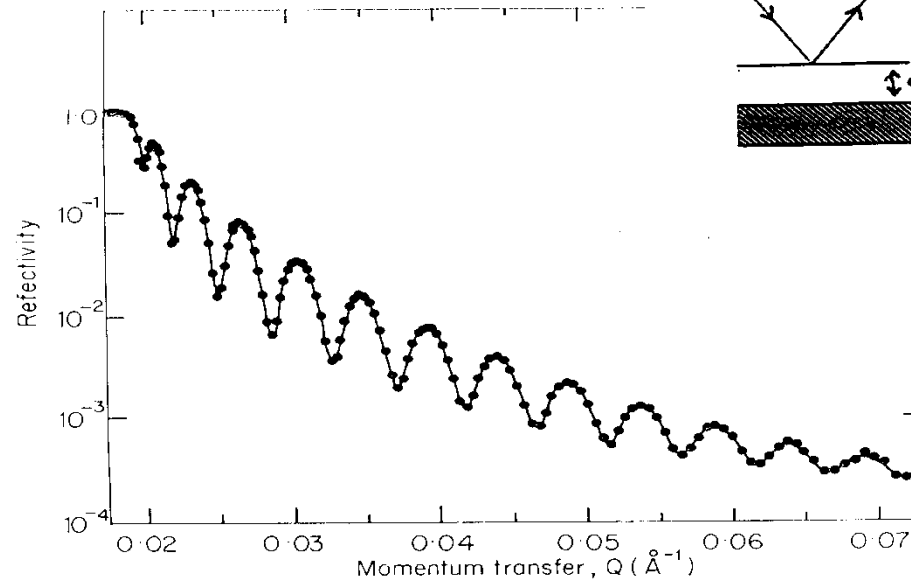
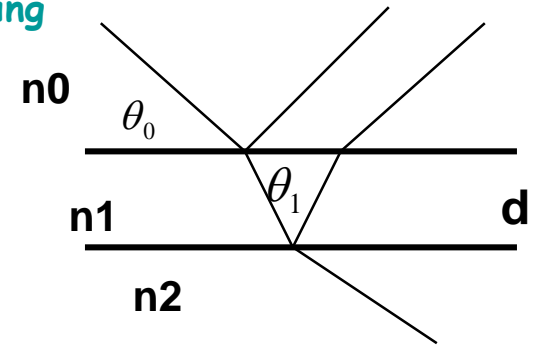
For a single thin film at an interface

$$R(Q) = \left| \frac{r_{01} + r_{12}e^{-2i\beta}}{1 + r_{01}r_{12}e^{-2i\beta}} \right|^2$$

$$r_{ij} = \frac{p_i - p_j}{p_i + p_j}$$

$$p_i = n_i \sin \theta$$

$$\beta_i = \frac{2\pi}{\lambda} n_i d_i \sin \theta_i$$



For a single thin film :

$$R(Q) = \frac{r_{01}^2 + r_{12}^2 + 2r_{01}r_{12} \cos 2n_1 k_1 d_1}{1 + r_{01}^2 r_{12}^2 + 2r_{01}r_{12} \cos 2n_1 k_1 d_1}$$

For $Q \gg Q_c$:

$$R(Q) \sim \frac{16\pi^2}{Q^4} \left[(\rho_1 - \rho_0)^2 + (\rho_2 - \rho_1)^2 + 2(\rho_1 - \rho_0)(\rho_2 - \rho_1) \cos(Qd) \right]$$

Fourier transform of 2 delta functions (young's slits)

FRINGE SPACING :

$$\Delta Q = \frac{2\pi}{d}$$

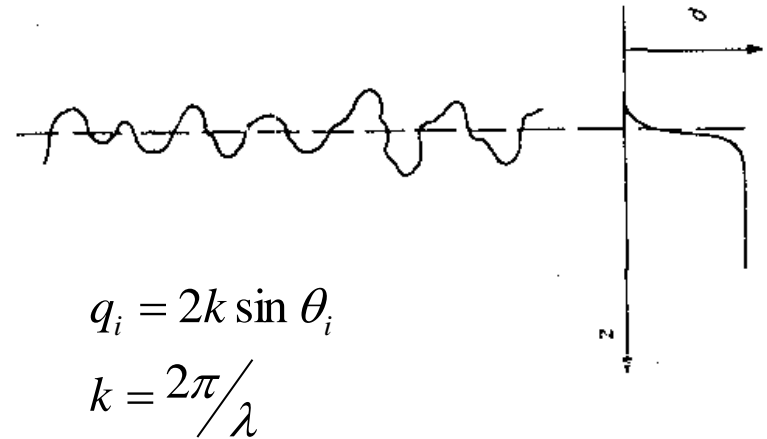
Rough or Diffuse Interface

For a simple interface reflectivity modified by,

$$R = R_0 \exp(-q_0 q_1 \sigma^2)$$

σ is rms Gaussian roughness

Gaussian factor (like Debye-Waller factor) results in larger than q^{-4} dependence in the reflectivity.



$$q_i = 2k \sin \theta_i$$

$$k = 2\pi/\lambda$$

(Nevot, Croce, Rev Phys Appl 15 (1980) 125, Sinha, Sirota, Garoff, Stanley, Phys Rev B 38 (1988) 2297)

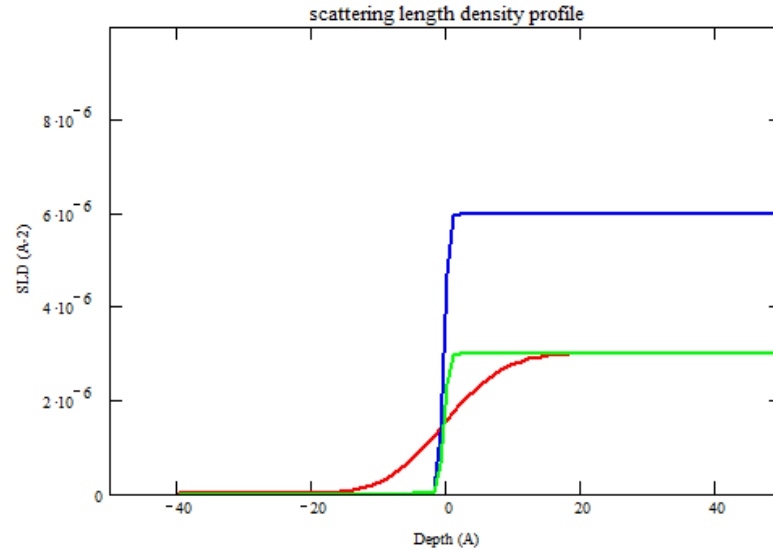
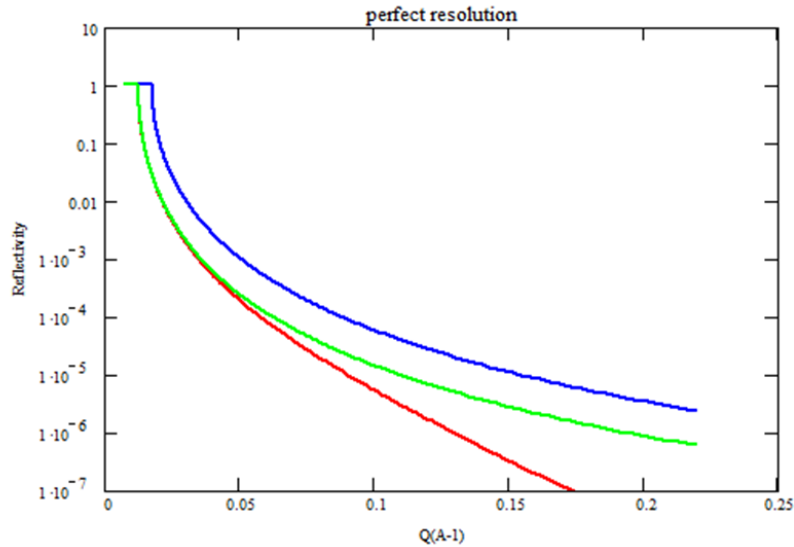
Can be also applied to reflection coefficients in formulism for thin films,

$$r_{ij} = \frac{(p_i - p_j)}{(p_i + p_j)} \exp(-0.5(q_i q_j \sigma^2))$$

From specular reflectivity cannot distinguish between roughness and diffuse interface



Reflectivity from a simple interface



Effect of roughness and sld

Glass optical flat

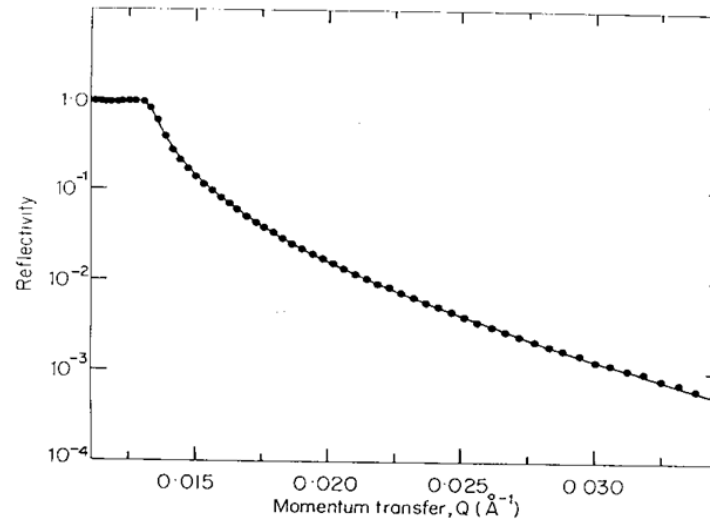
$$\theta = 0.35$$

$$Nb = 0.35 \times 10^{-5} \text{ \AA}^{-2}$$

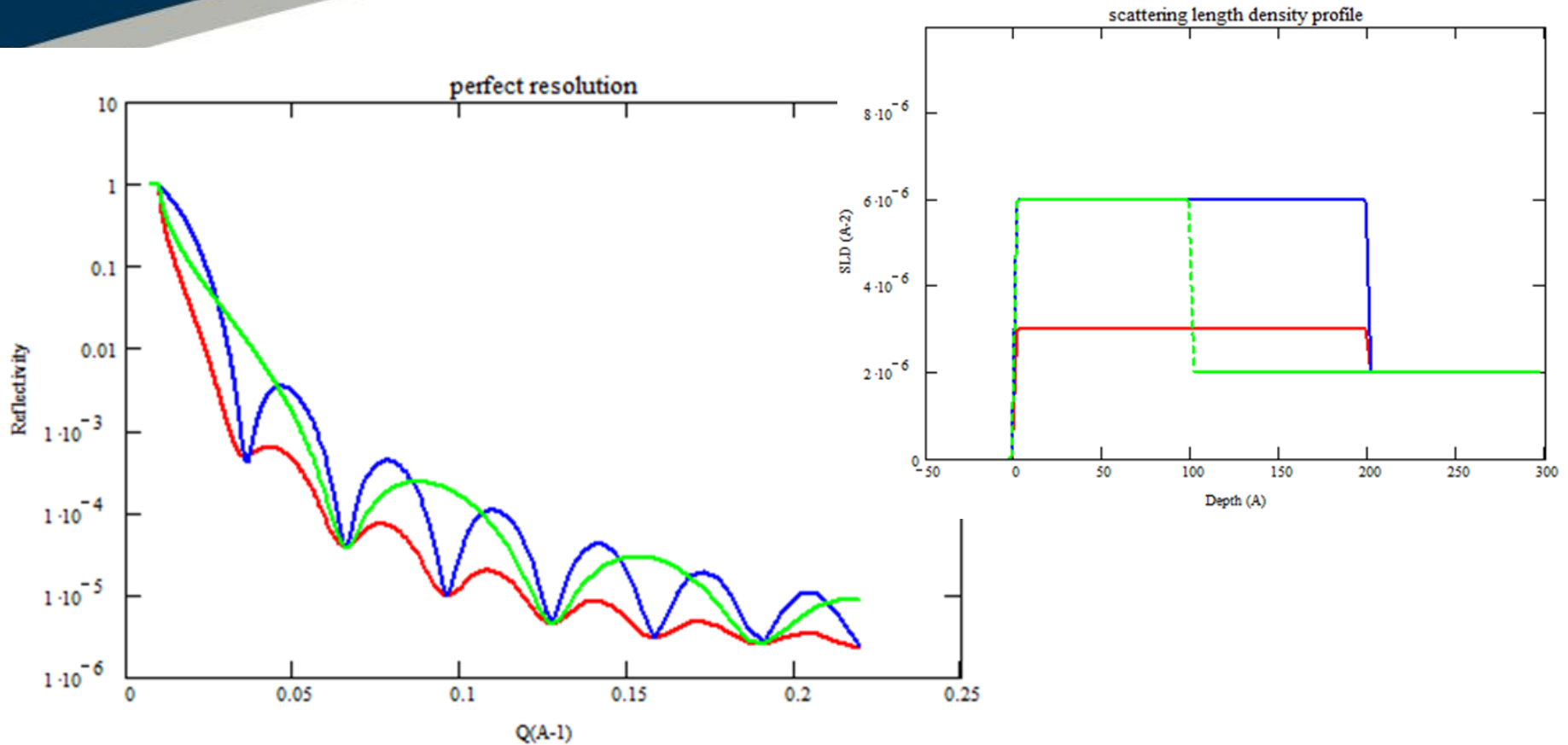
$$\sigma = 33 \text{ \AA}$$

$$\Delta\theta = 5\%$$

Penfold & Thomas
1990

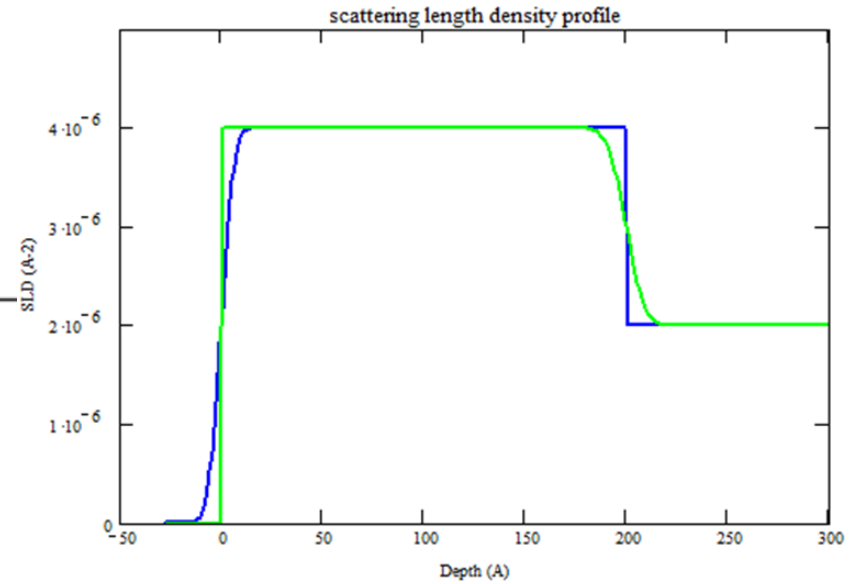
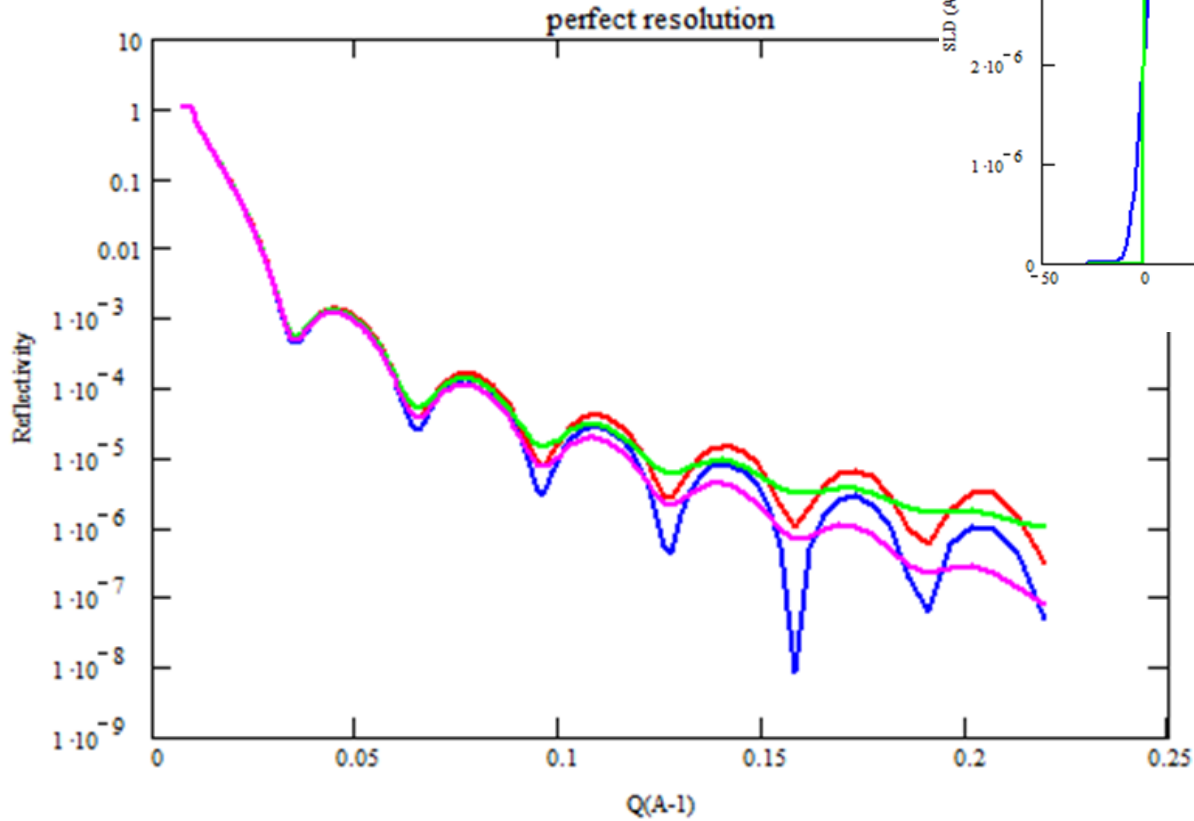


Reflectivity from thin films



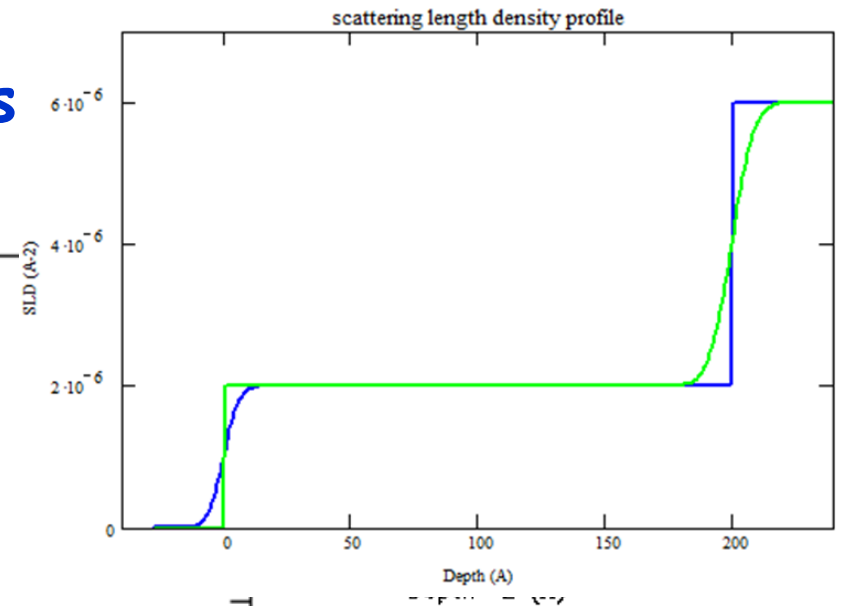
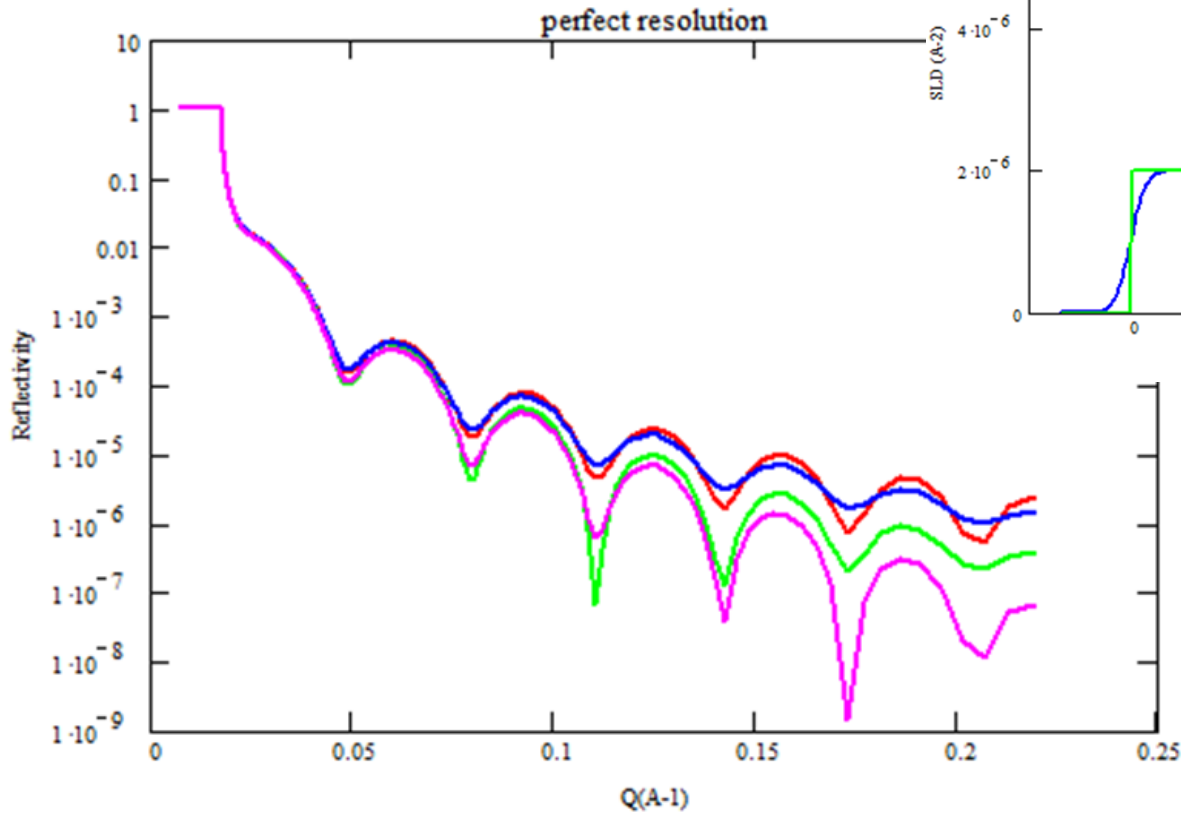
Effect of film thickness and refractive index

Reflectivity from thin films



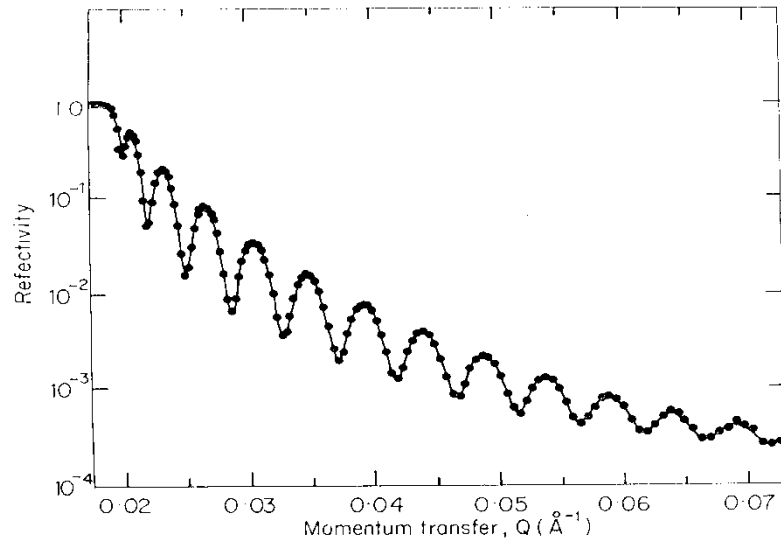
Effect of interfacial roughness

Reflectivity from thin films



Effect of interfacial roughness

Reflectivity from a thin film



Deuterated L-B film on silicon

$$d = 1198 \text{ \AA}$$

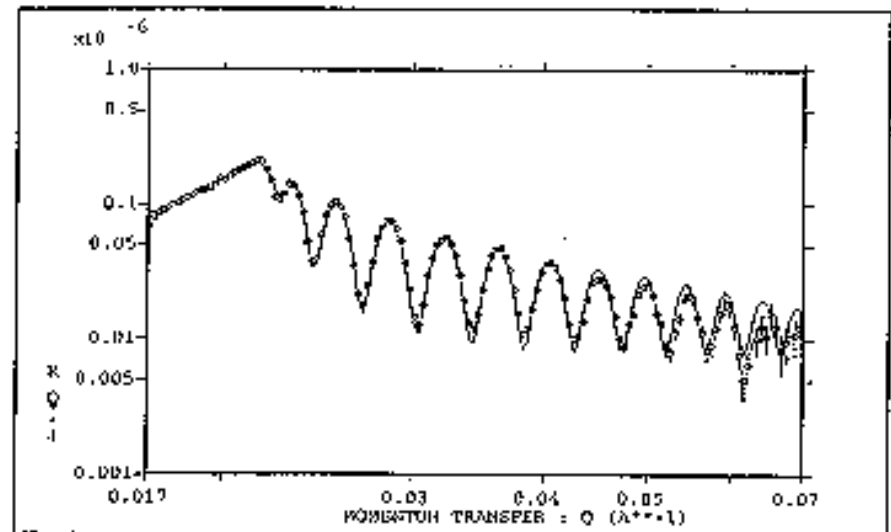
$$Nb = 0.74 \times 10^{-5} \text{ \AA}^{-2}$$

$$\theta = 0.5, \Delta\theta = 4\%, \sigma = 20 \text{ \AA}$$

NiC film on silicon

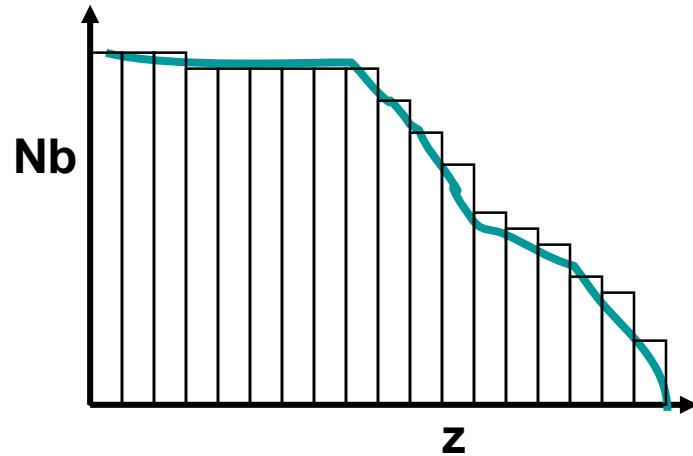
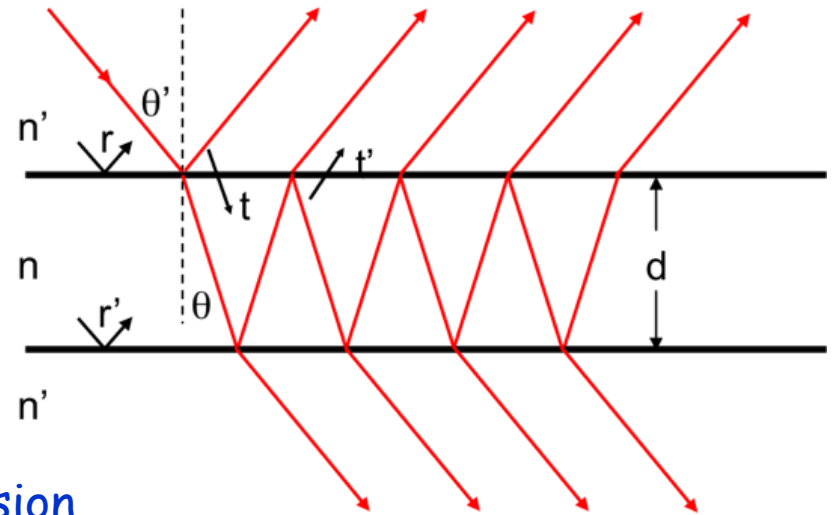
$$d = 1194 \text{ \AA}, Nb = 0.94 \times 10^{-5} \text{ \AA}^{-2}$$

$$\theta = 0.5, \Delta\theta = 4\%, \sigma_1 = 10, \sigma_2 = 15 \text{ \AA}$$



Reflection from more complex interfaces (multiple layers)

Airy's fomula (Parratt)



Combination of reflection and transmission coefficients give amplitude of successive beams reflected,

$$r_1, t_1 t_1' r_2, -t_1 t_1' r_1 r_2^2, t_1 t_1' r_1^2 r_2^3 \text{ and so on}$$

(Parratt, Phys Rev 95 91954) 359
G B Airy, Phil Mag 2 (1833) 20)

Phase change on traversing film, $\delta_1 = \frac{2\pi}{\lambda} n_1 d_1 \sin \theta_1$

$$R = r_1 + t_1 t_2' r_2 e^{-2i\delta_1} - t_1 t_1' r_1 r_2^2 e^{-4i\delta_1} + \dots$$

More general matrix formulisms (Born & Wolf, Abeles) available

Reflection from multiple layers

Born and Wolf matrix formalism

Applying conditions that wave functions and their gradients are continuous at each boundary gives rise to a **Characteristic matrix** per layer,

$$M_j = \begin{bmatrix} \cos \beta_j & -(i/p_j) \sin \beta_j \\ -ip_j \sin \beta_j & \cos \beta_j \end{bmatrix}$$

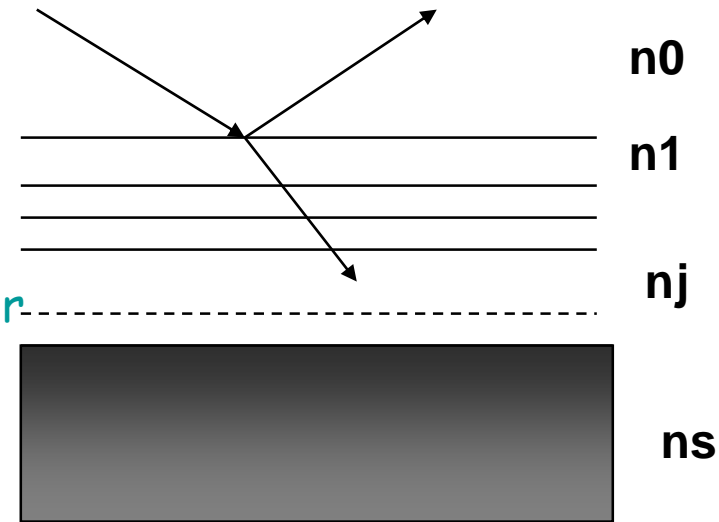
$$p_j = n_j \sin \theta_j$$

$$\beta_j = (2\pi/\lambda)n_j d_j \sin \theta_j$$

$$M_R = [M_1][M_2] \dots [M_n]$$

The resultant reflectivity is

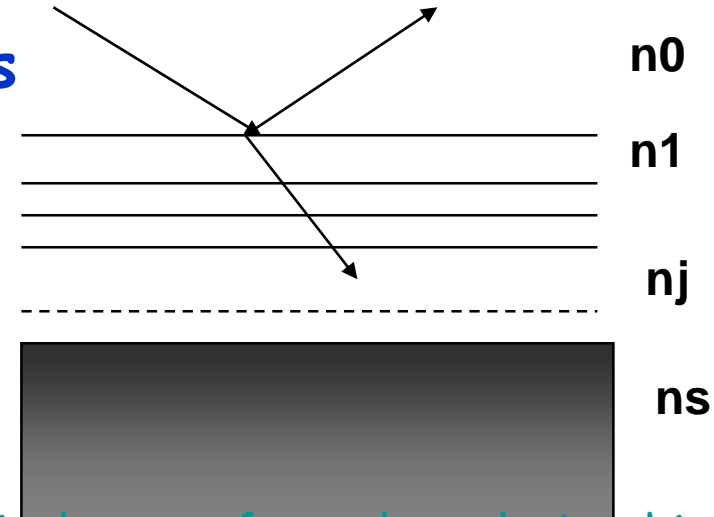
$$R = \left[\frac{(M_{11} + M_{12}p_s)p_a - (M_{21} + M_{22})p_s}{(M_{11} + M_{12}p_s)p_a + (M_{21} + M_{22})p_s} \right]^2$$



(Born & Wolf, 'Principles in Optics',
6th Ed, Pergamon, Oxford, 1980)

Reflection from multiple layers

In Born and Wolf approach can only include roughness / diffusiveness at interfaces by further sub-division in small layers.



Abeles method, using reflection coefficients overcomes this limitation

Define characteristic matrix per layer, in optical terms from the relationship between electric vectors in successive layers,

$$C_j = \begin{bmatrix} e^{i\beta_{j-1}} & r_j e^{i\beta_{j-1}} \\ r_j e^{-i\beta_{j-1}} & e^{-i\beta_{j-1}} \end{bmatrix}$$

$$[C_1] \cdot [C_2] \cdots [C_{n+1}] = \begin{bmatrix} a & b \\ c & d \end{bmatrix}$$

To include roughness,

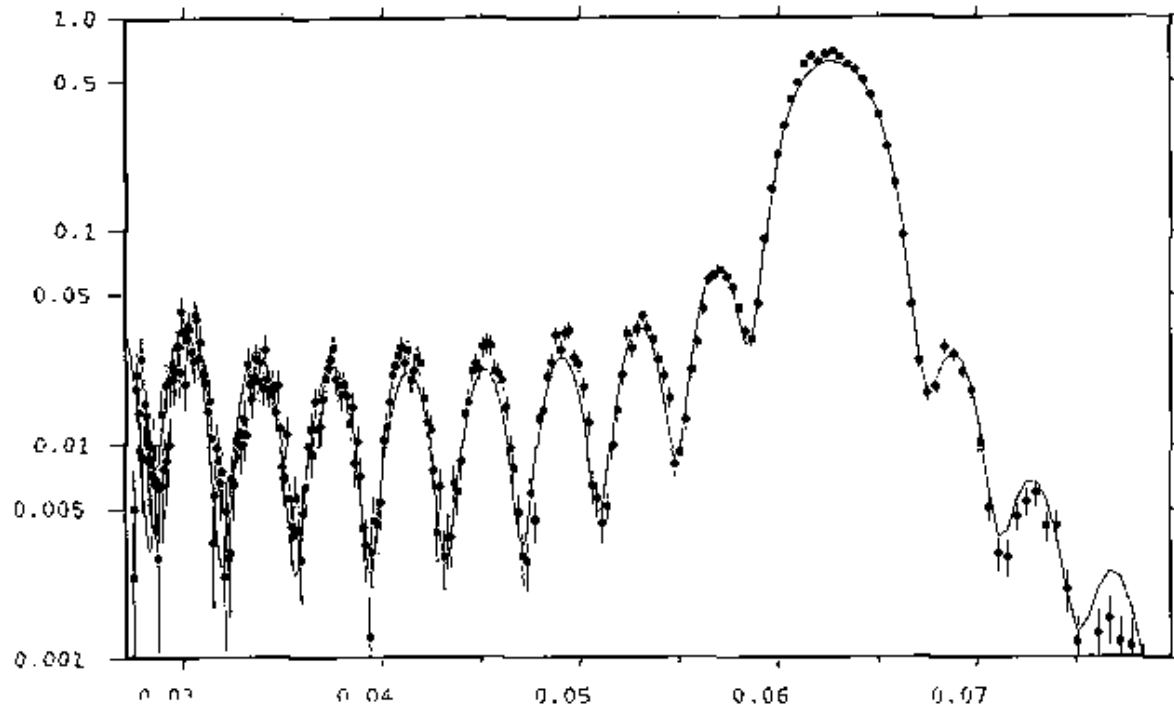
$$r_j = \frac{(p_{j-1} - p_j)}{(p_{j-1} + p_j)} \exp(-0.5q_j q_{j-1} \sigma^2)$$

(Heavens, 'Optical properties of solid thin films', Butterworths, London, 1955, F Abeles, *Annale de Phys* 5 (1950) 596)

The resultant Reflectivity is then,

$$R = CC^* / AA^*$$

Multiple Layer films

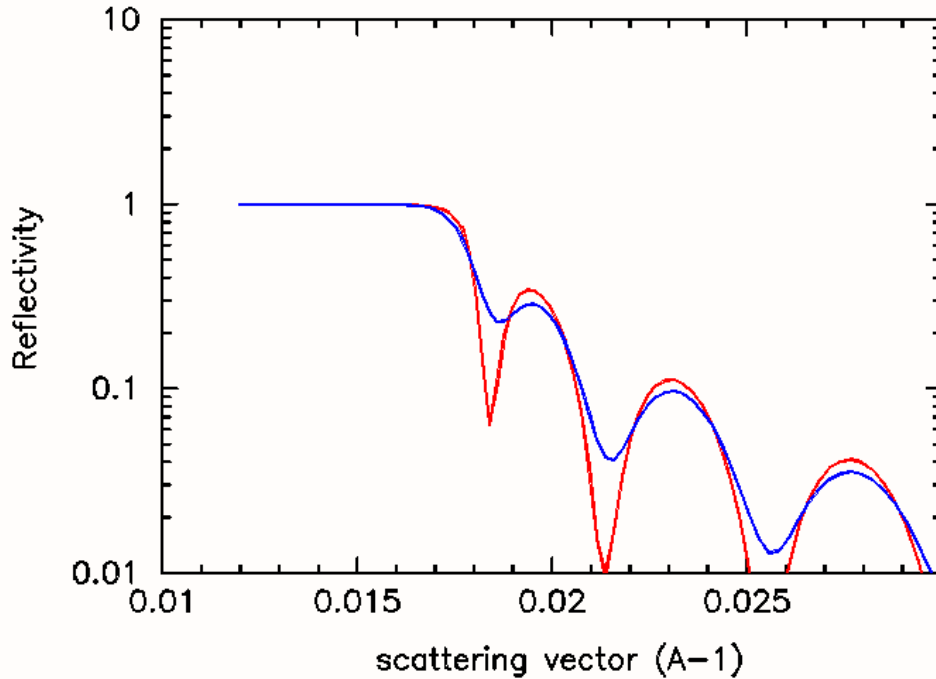


Region around 1st order Bragg peak for Ni/Ti multilayer
15 bilayers (46.7, 1.0×10^{-5} / 55.7, -0.13×10^{-5})

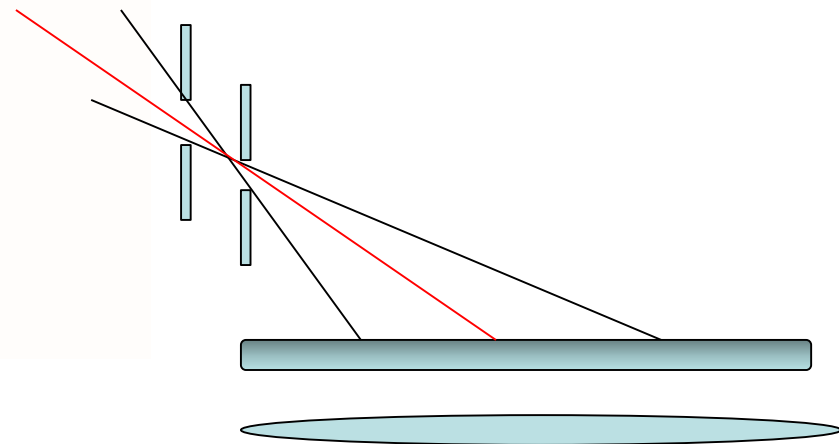


Effects of resolution

$$\frac{\Delta Q^2}{Q^2} = \frac{\Delta t^2}{t^2} + \frac{\Delta \theta^2}{\theta^2}$$



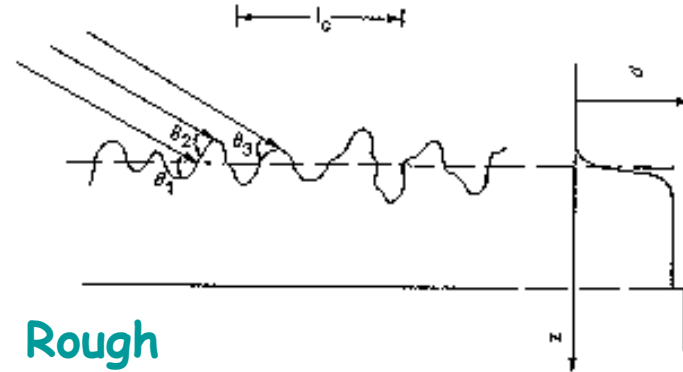
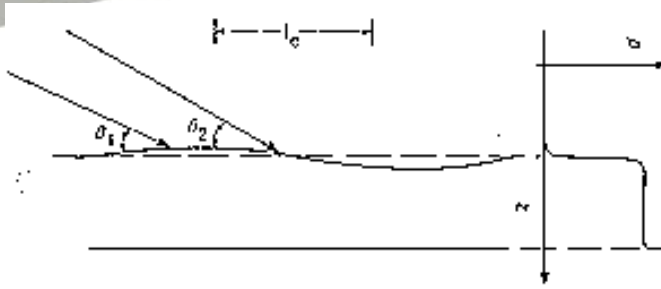
On ISIS reflectometers resolution is dominated by collimation



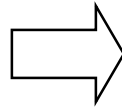
1000 \AA film on Si , $\Delta Q/Q$ 2%, 6%

Damps interference fringes, rounds critical edge

Surface roughness and Waviness

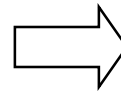


Curvature > coherence length



Rough

Curvature < coherence length



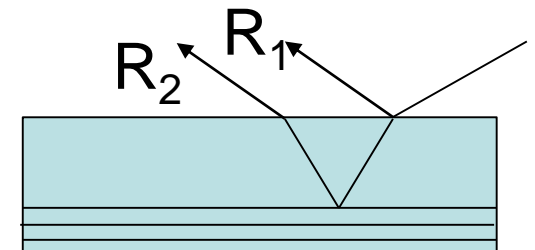
Waviness

This initially has an effect similar to resolution, and in the extreme can be treated by geometrical optics.

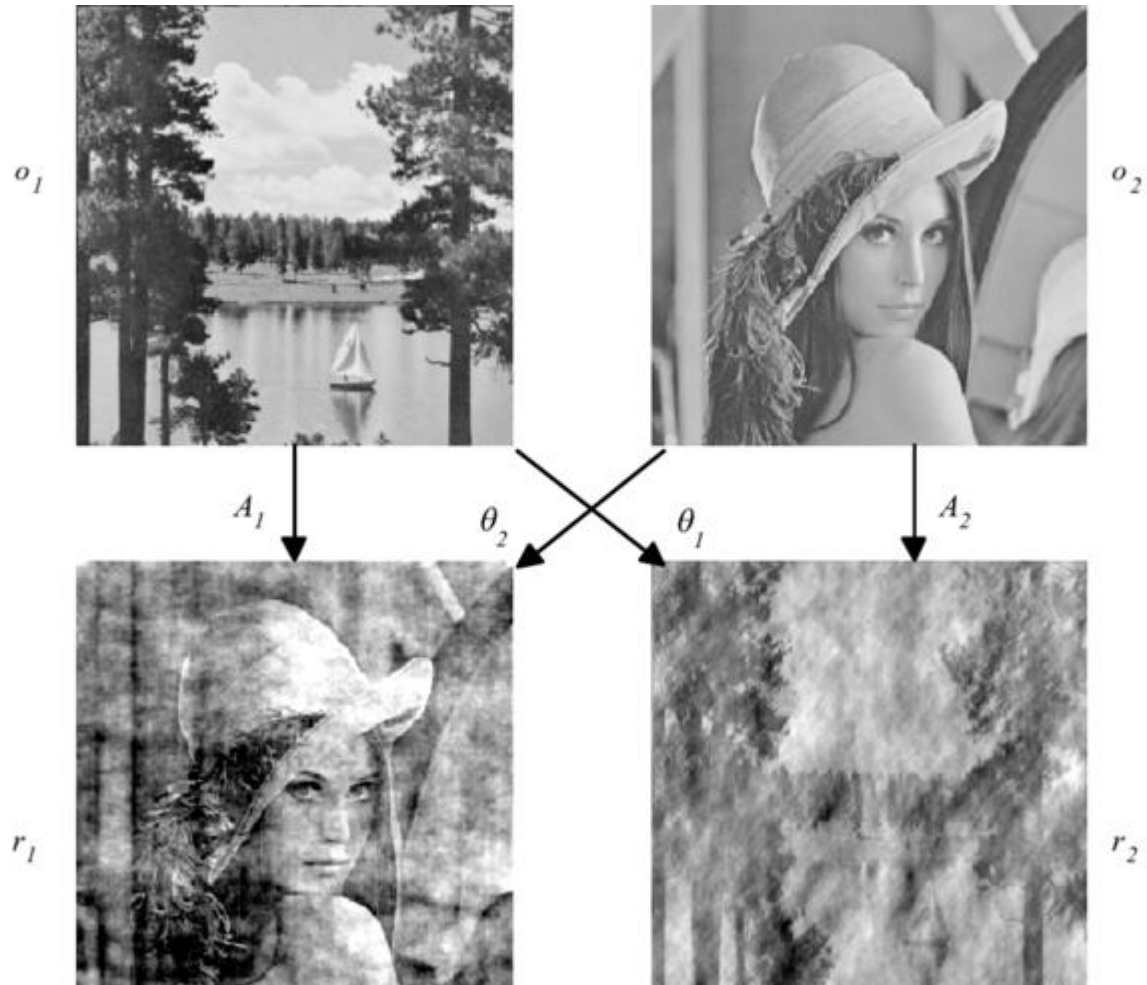
Incoherent reflectivity from 2 surfaces, separated by an adsorbing media:

$$R_{tot}(Q) = R_1(Q) + \frac{(1 - R_1(Q))^2 R_2(Q) A(Q)}{1 - R_1(Q) R_2(Q) A(Q)}$$

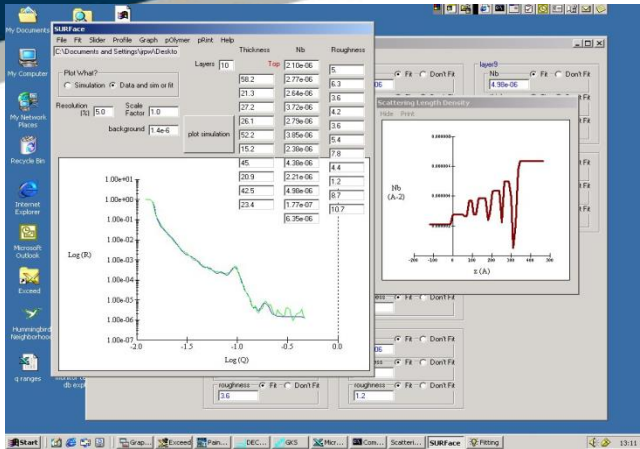
Thickness > coherence length
 $A(Q) \sim$ Beer-Lambert



Loss of Phase Information



Model fitting Reflectivity data



reflectivity $\xrightarrow{\text{Scattering length density}}$

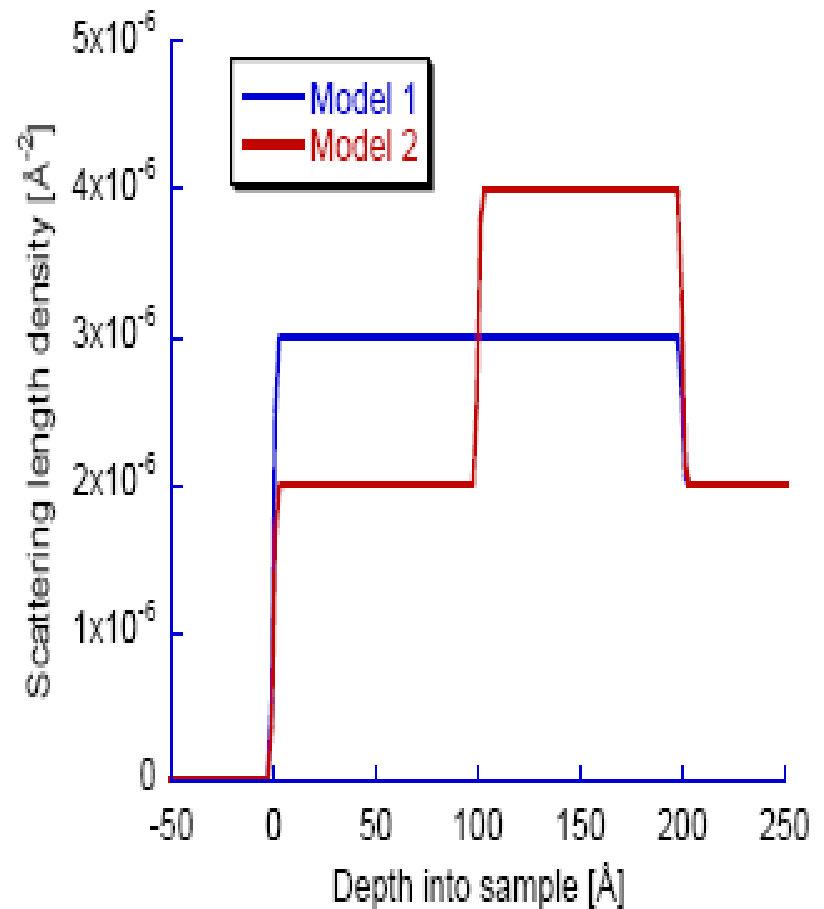
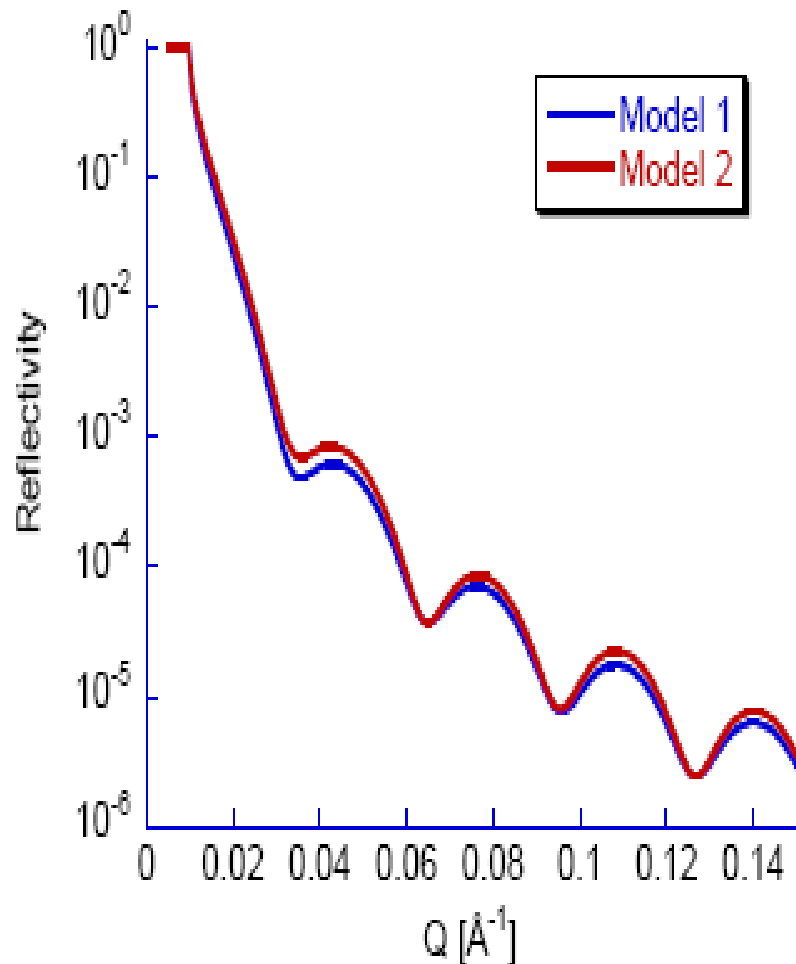
- Uniqueness ?
- Resolution ?
- Model dependent / over interpretation of data ?
- Does the scattering length density profile give access to the necessary physical parameters (Intra molecular) ?

Steepest decent, simplex,
 simulated annealing,
 genetic, cubic spline + fft,
 etc etc

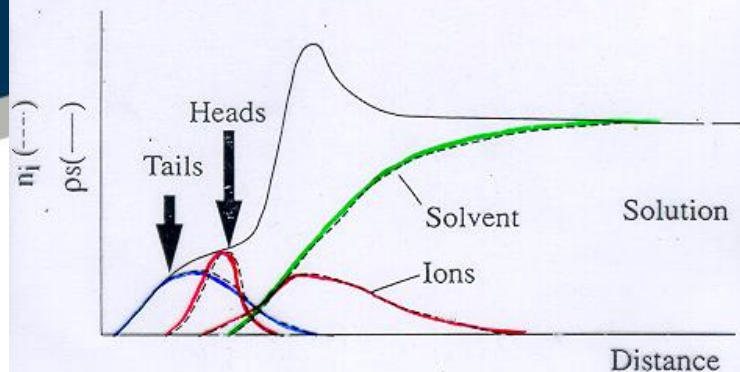


Lateral (z) and rotational
 invariance

Perils of fitting



Partial Structure Factors



$$R(Q) = \frac{16\pi^2}{Q^2} \left| \int_{-\infty}^{+\infty} \rho(z) e^{-iQz} dz \right|^2$$

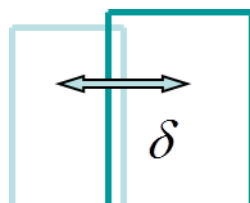
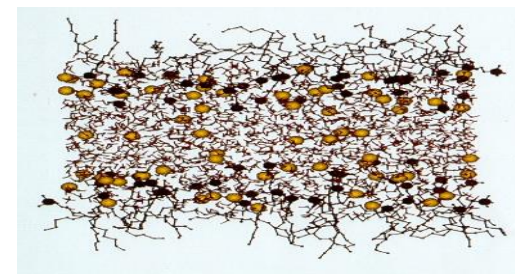
$$\rho(z) = b_c n_c(z) + b_h n_h(z) + b_s n_s(z)$$

$$R(Q) = \frac{16\pi^2}{Q^2} [b_c^2 h_{cc} + b_h^2 h_{hh} + b_s^2 h_{ss} + 2b_c b_h h_{ch} + 2b_c b_s h_{cs} + 2b_h b_s h_{hs}]$$

Self Partial Structure Factors : $h_{ii} = |\hat{n}_i|^2$

\hat{n}_i is a one dimensional Fourier transform of $n_i(z)$

Cross partial structure factors:



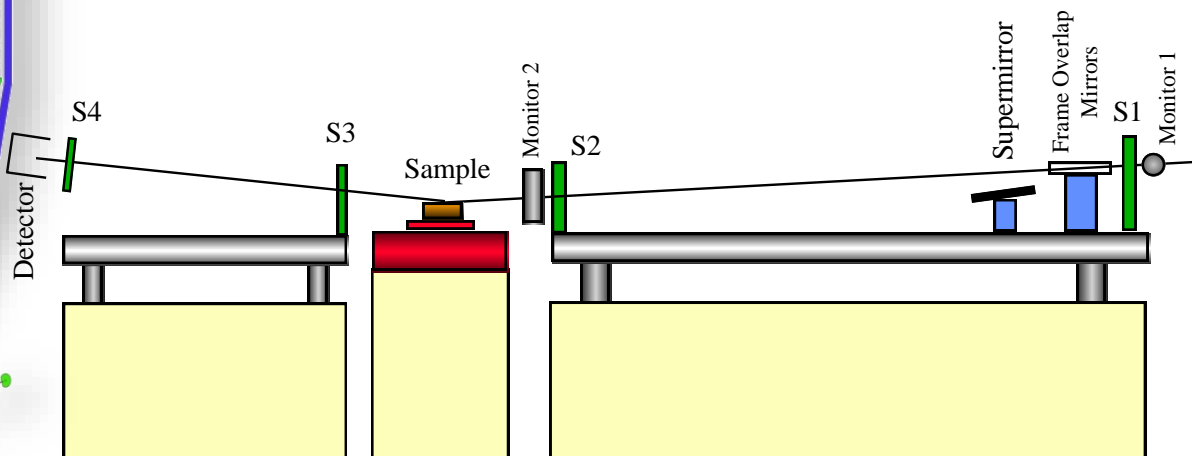
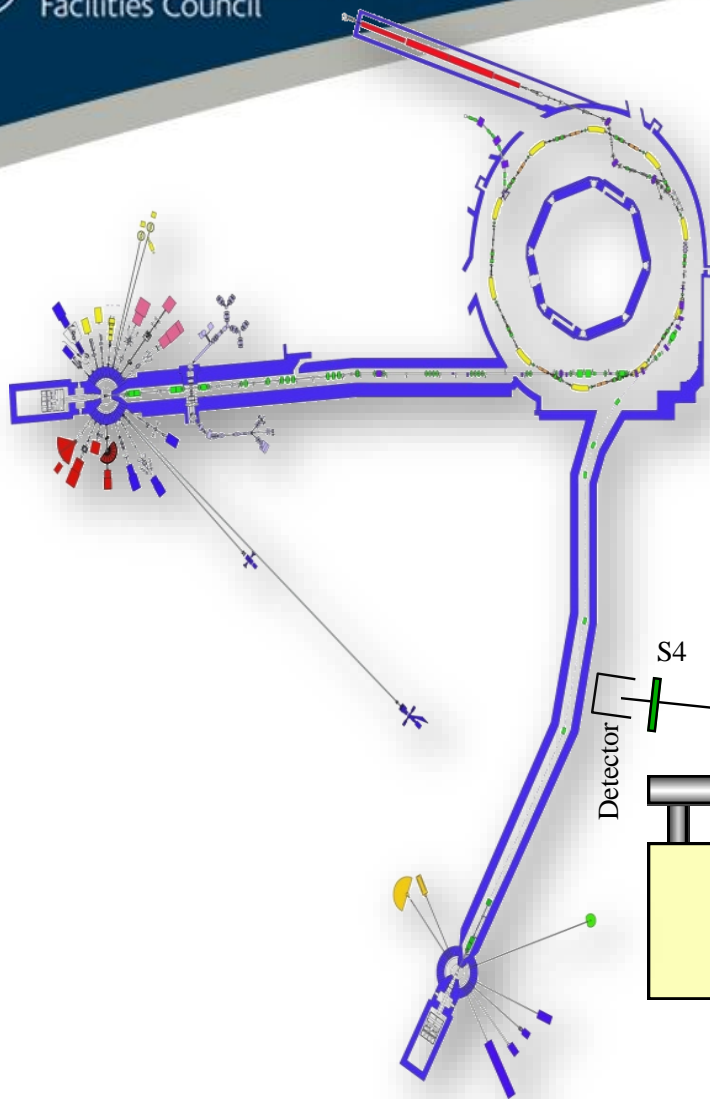
$$h_{ij} = \pm [h_{ii} h_{jj}]^{1/2} \cos iQ\delta$$

(Crowley, Lee, Simister, Thomas, Penfold, Rennie,
Coll Surf 52 (1990) 85)

Neutron Reflectivity at ISIS

Measure variation of reflectivity
with scattering vector, Q_z ,
perpendicular to the interface

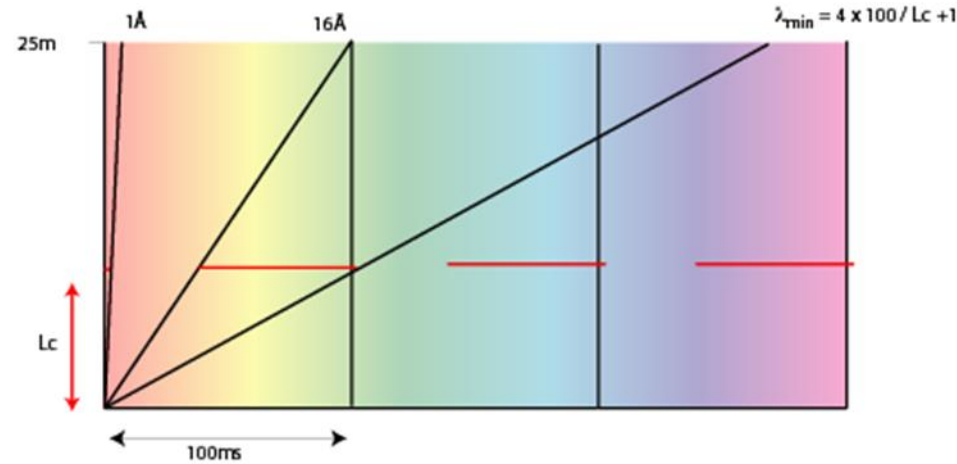
Using 'white beam' TOF method
with fixed angle and range
of wavelengths



**INTER, POLREF, OFFSPEC,
SURF, CRISP reflectometers**

(Penfold, Williams, Ward, *J Phys E* 20 91987) 1411; J Penfold et al,
J Chem Soc, Faraday Trans, 94 (1998) 955

Instrumentation



White beam time of flight, fixed geometry: Wavelength range 1-7(16)Å
Q range 3×10^{-3} to 0.5 \AA^{-1}

Q_{\max} (d_{\min}) limited by background:

incoherent scattering in sample
 1.5×10^{-6} for D₂O, 4×10^{-6} for H₂O
 $< 10^{-6}$ for silicon

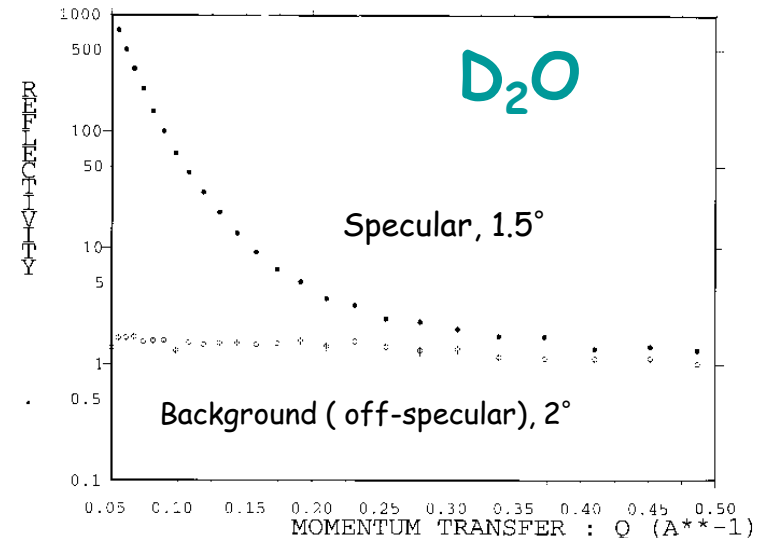
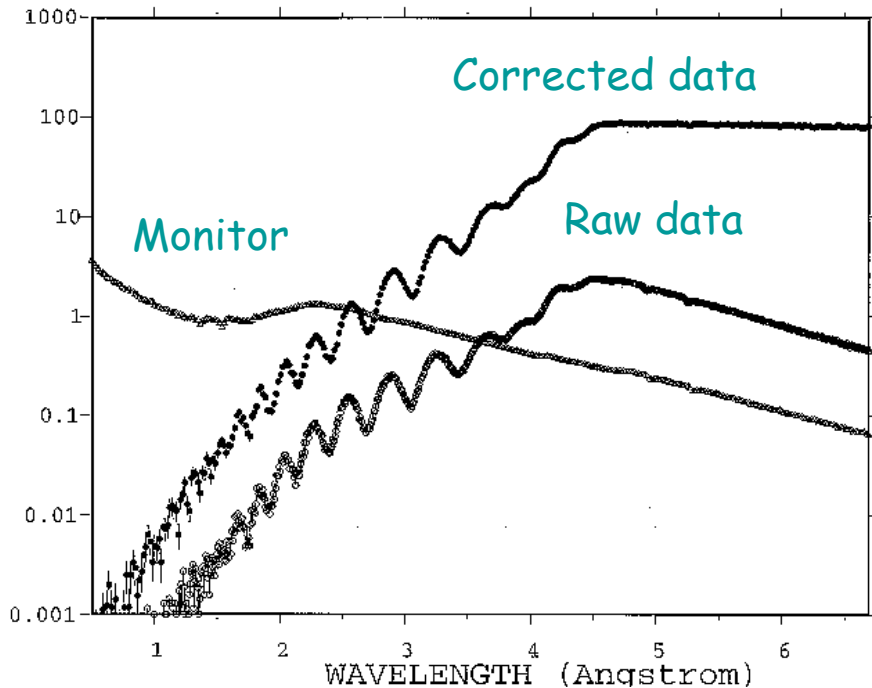
d_{\max} determined by $\Delta Q/Q$

Instrumentation

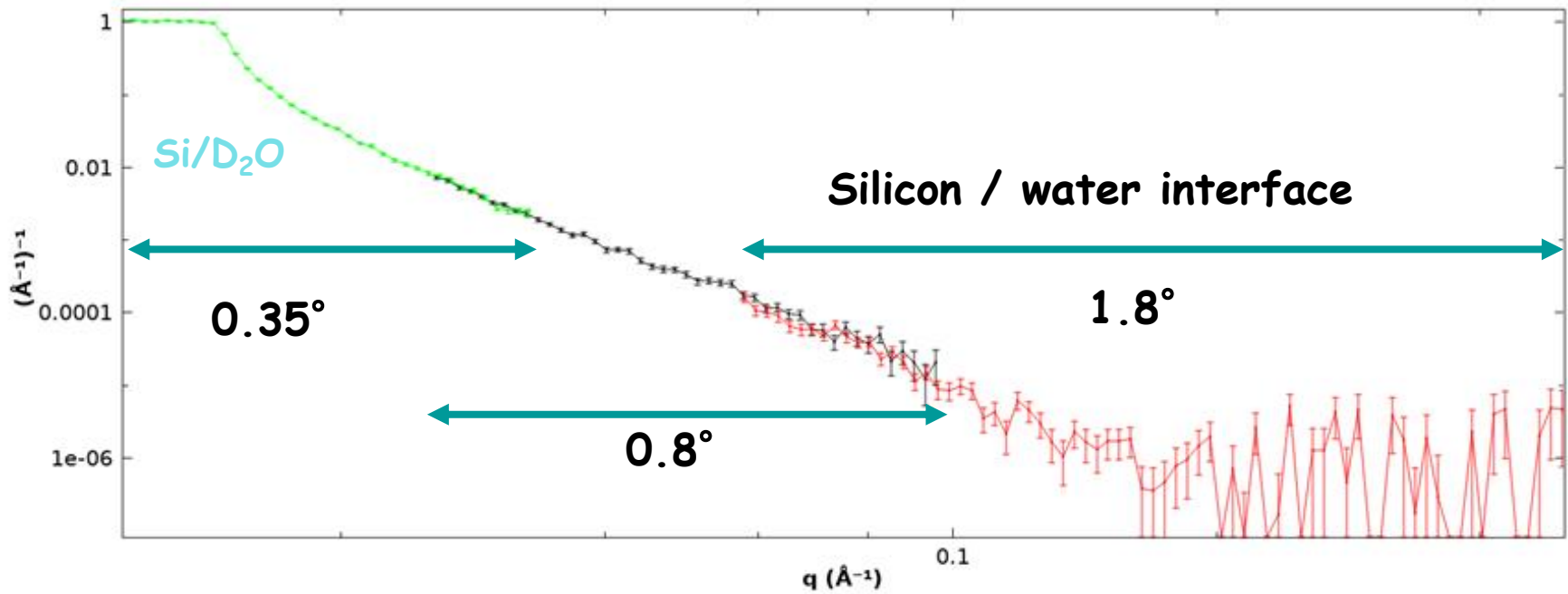
Correct for detector efficiency,
spectral shape, background

$$R(Q(\lambda_i, \theta)) = f \frac{[I_d(\lambda_i) - b_d(\lambda_i)] \varepsilon_m(\lambda_i)}{[I_m(\lambda_i) - b_m(\lambda_i)] \varepsilon_d(\lambda_i)}$$

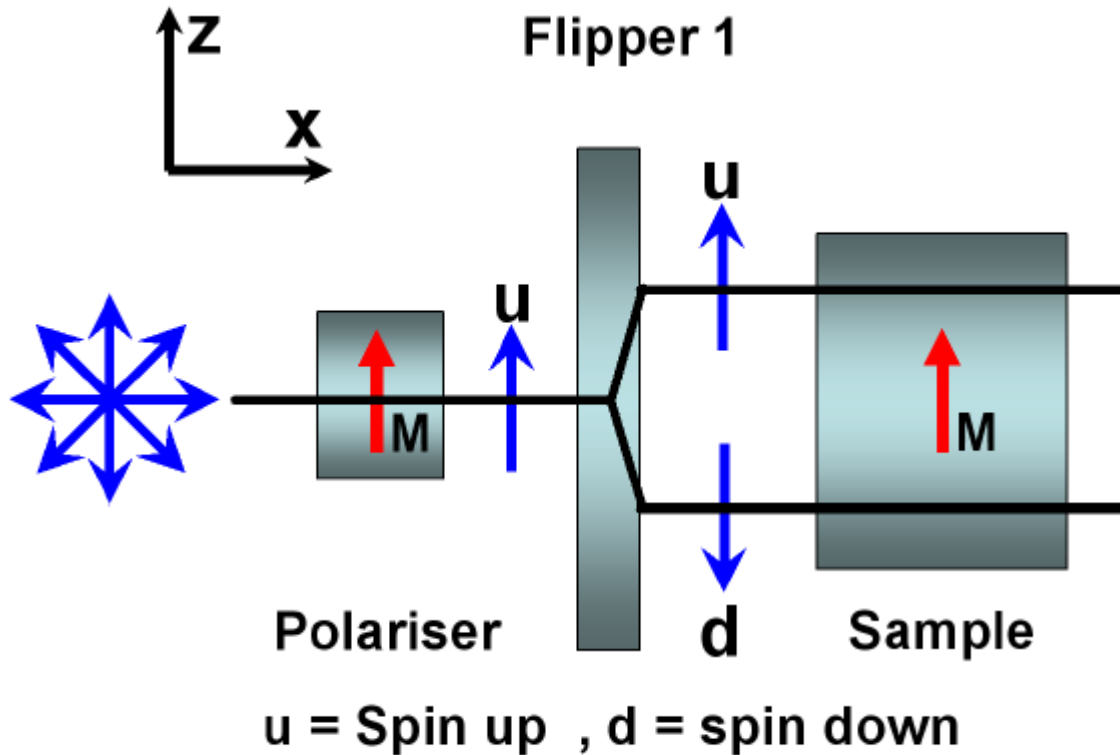
d,m refer to the detector and monitor
m can also be a direct beam



Instrumentation



Polarised neutrons

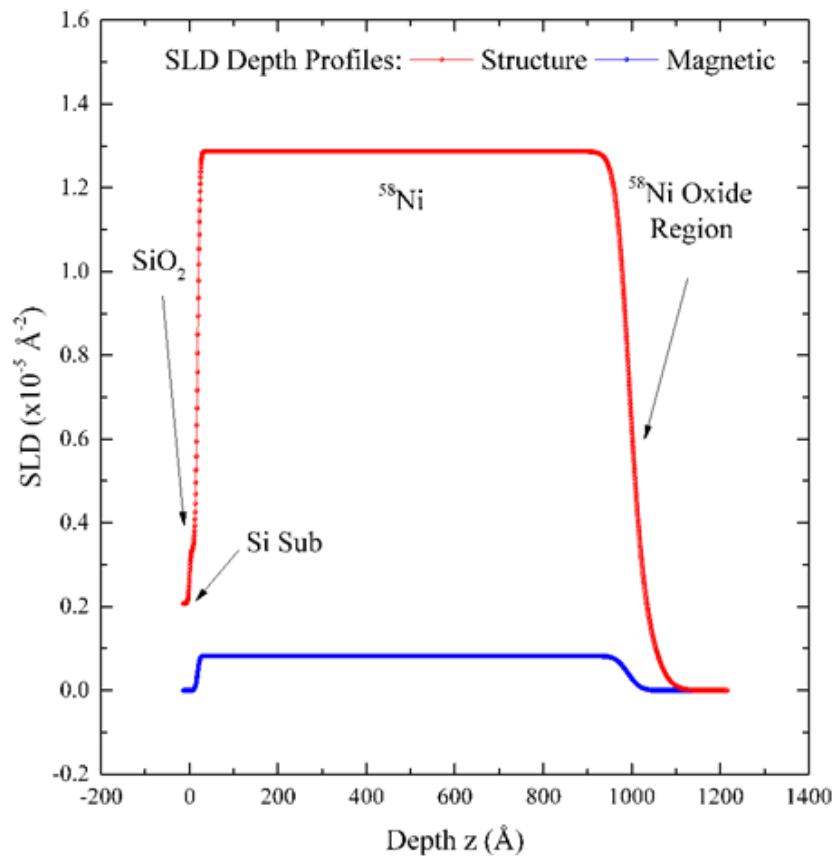
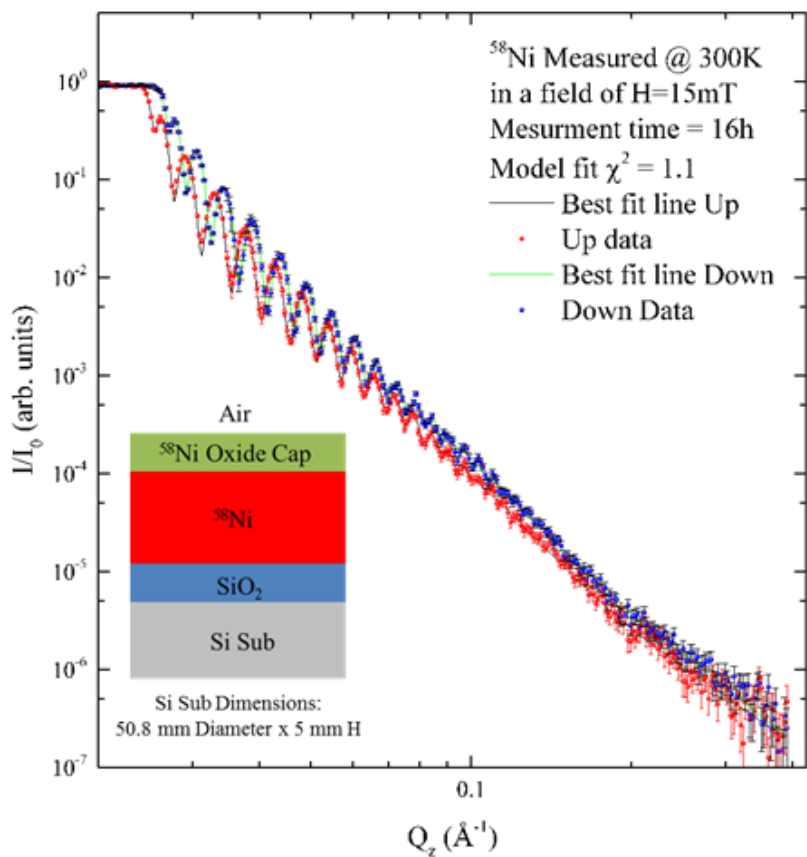


Now measure to reflectivity curves spin up and spin down.

Experiments now takes 4 times as long to get similar statistics!

There several ways of polarising and flipping neutrons, but that is beyond scope of this talk.

Example of Polarised Neutron Reflectivity (PNR)



PNR provides both the Nuclear (structural) and magnetic SLD depth profile.

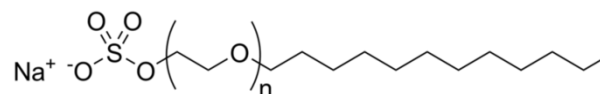
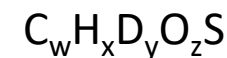
Effectively functions as a depth dependent magnetometer

But takes longer than NR by a factor 4 for similar statistics



Simple determination of surface excess (how much stuck to surface/interface)

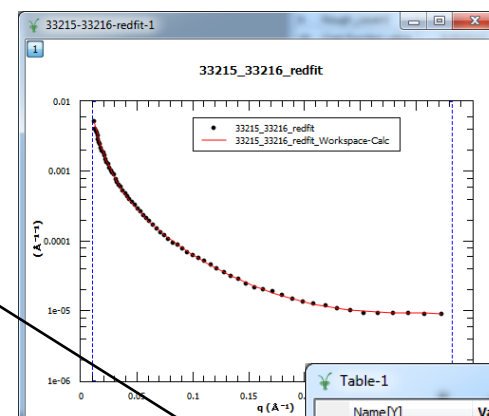
Air Contrast Matched Water



$$A = \sum b / d\rho$$

$$\Gamma = 1 / A \cdot N_{av}$$

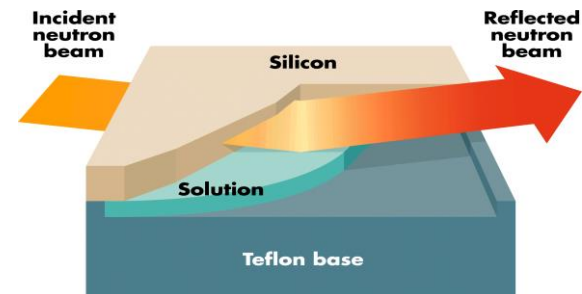
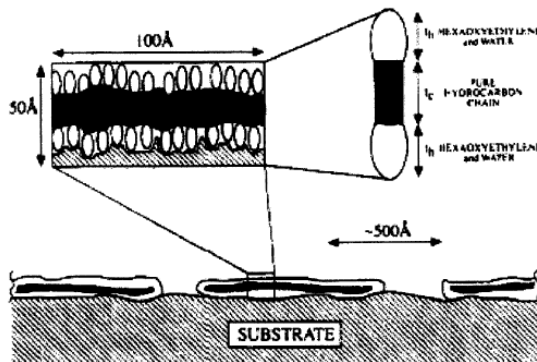
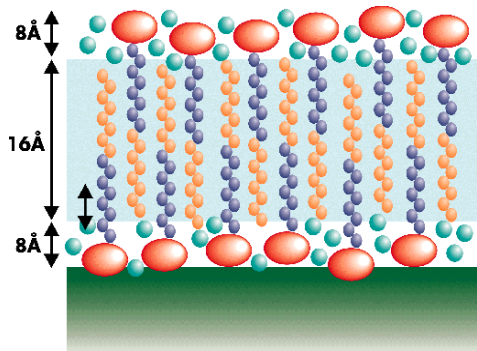
$$d\rho = \frac{\sum b_1}{A_1} + \frac{\sum b_2}{A_2}$$



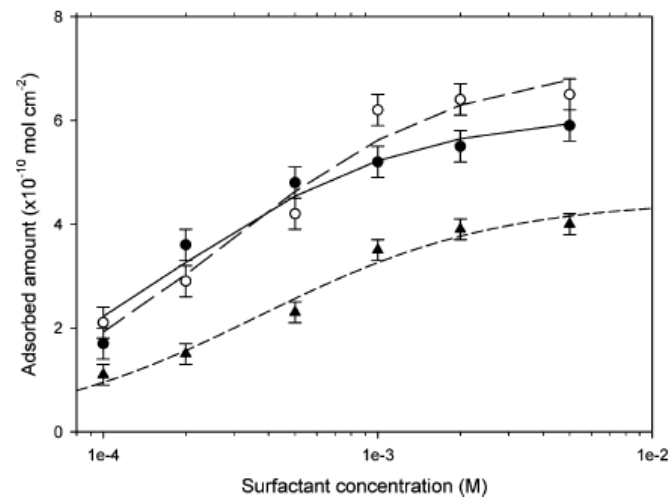
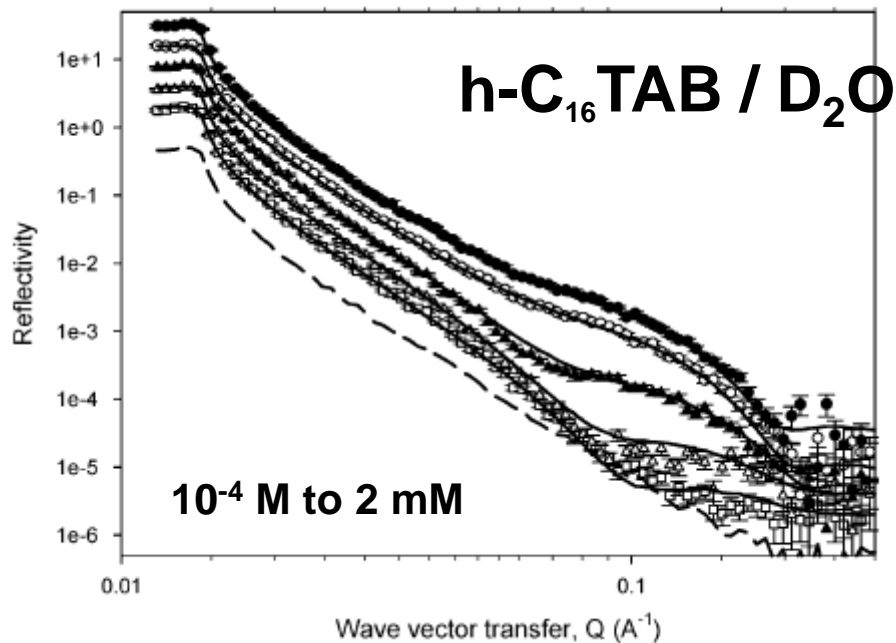
Name[Y]	Value[Y]	Error[Y]
0 Theta	2.3	0
1 ScaleFactor	1	0
2 AirSLD	0	0
3 BulkSLD	0	0
4 Roughness	0	0
5 Background	9.09315e-06	2.69601e-07
6 Resolution	5	0
7 SLD_Layer0	3.51781e-06	4.94563e-08
8 d_Layer0	19.6907	0.303912
9 Rough_Layer0	0	0
10 Cost function value	0.912111	0



Surfactant adsorption at the solid-solution interface

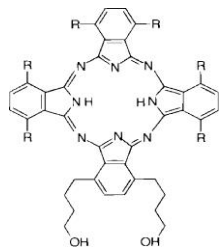


(●) silica, (○) phlic cellulose,
(Δ) phobic cellulose



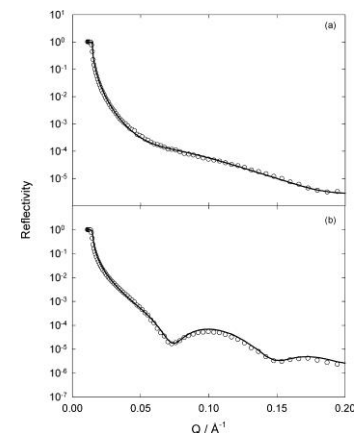
Optical biosensors

Principle: contaminants in water degrade lipid layer allowing release of trapped NO_2 causing colour change in pigment.

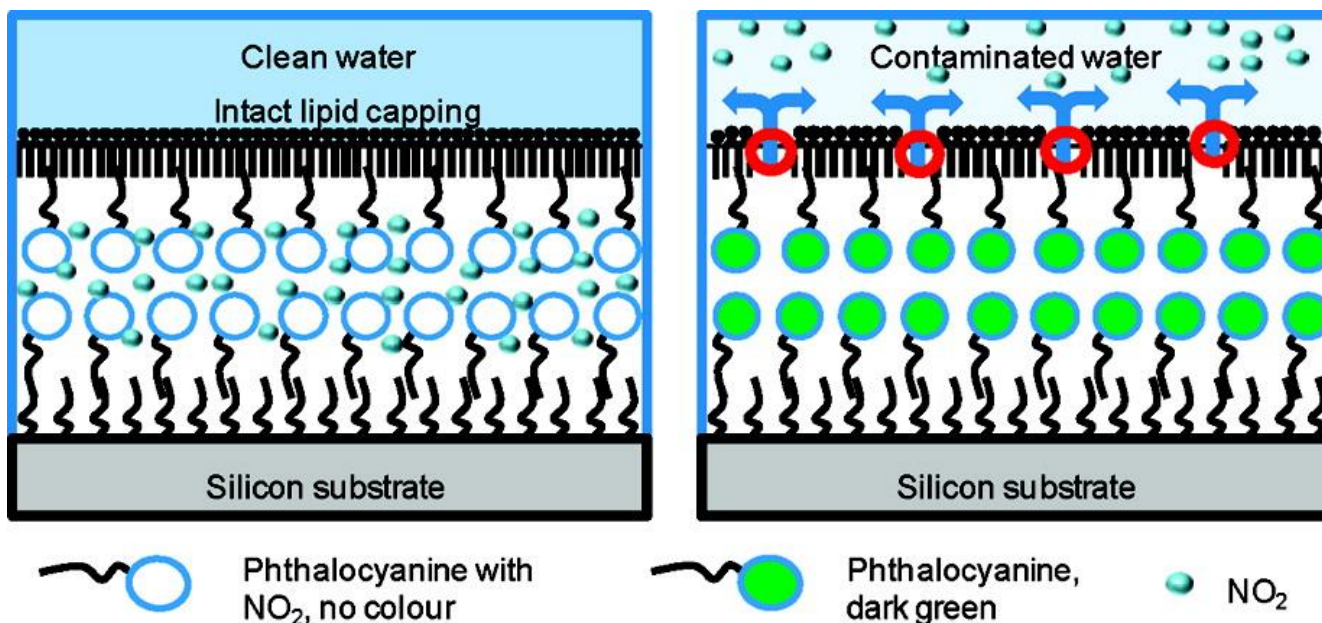


Chemical structure of the phthalocyanine ligand. The six R groups are $\text{C}_{10}\text{H}_{21}$.

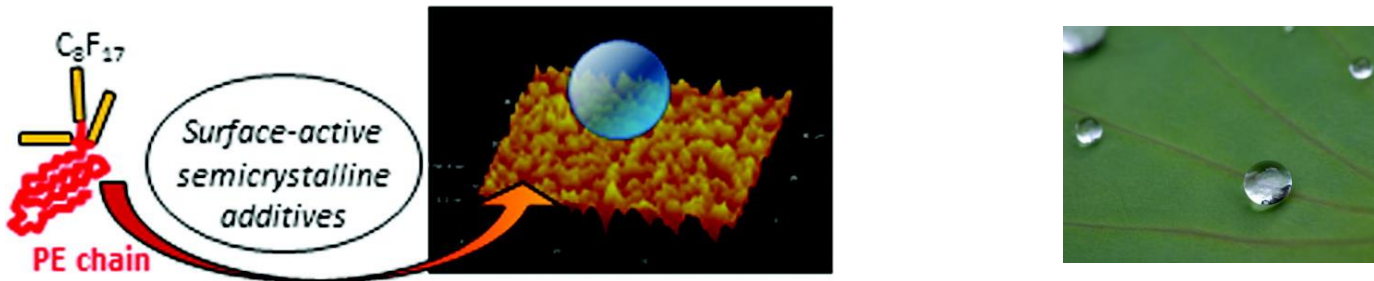
(a) Reflectivity profiles for DPPC-DPPE+PEG layer and (b) 2 layers of phthalocyanine covered by DPPC-DPPE+PEG at the silicon-D $_2$ O interface. The best fits to the data are shown by solid lines.



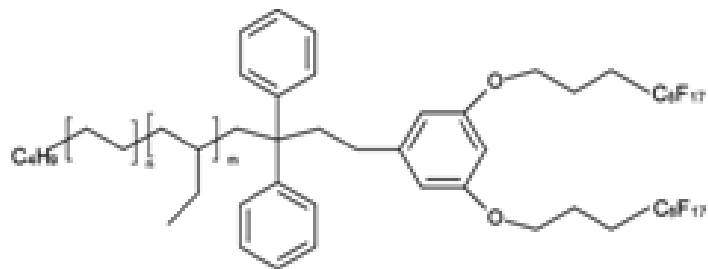
Reflectivity demonstrates effectiveness of the lipid layer in partitioning (sealing) the deposited phthalocyanine layers from the bulk water.



Surface Modification of Polyethylene with Multi-End-Functional Polyethylene Additives



- “New” surface properties for polymer films
- Polymer hydrophobicity greatly enhanced by end addition of fluorine
- Multi-end-fluorinated chain additives spontaneously surface enrich
- Suitable for one step batch process
- Marked increase in both hydrophobicity and lipophilicity
- PTFE like surface properties



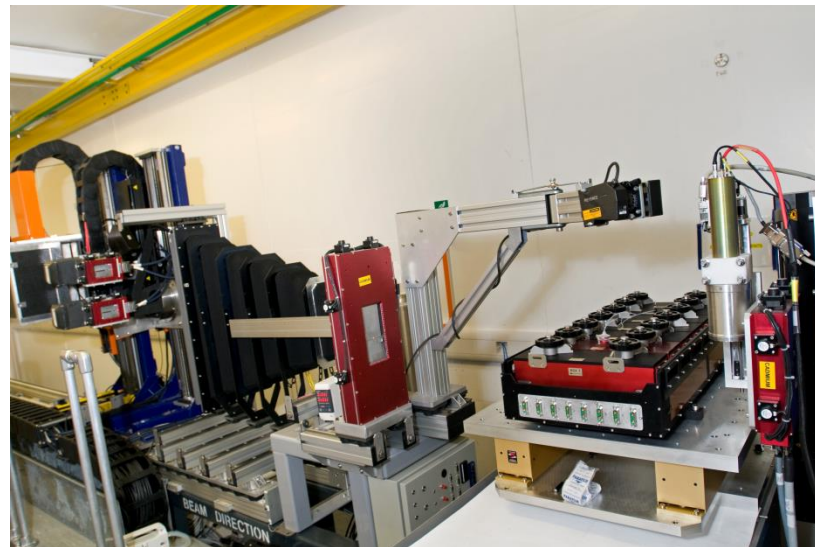
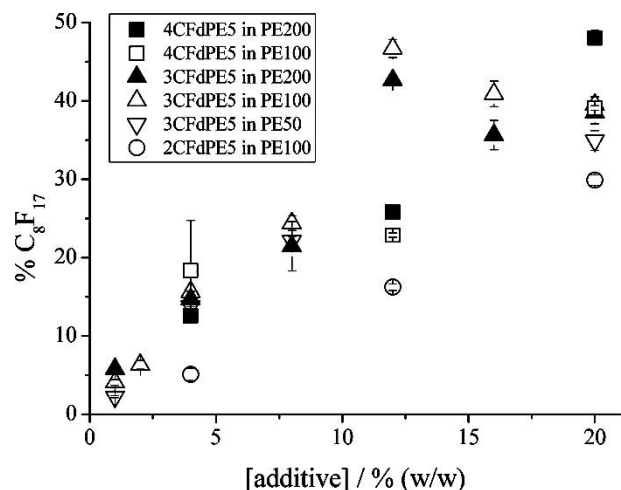
Additives made from polymerised 1,3 butadiene end capped with diphenyl ethylene and terminated with fluorinated aryl ether bromide followed by saturation with D₂ at 500 psi

sample code	target M _n /kg mol ⁻¹	measured M _n /kg mol ⁻¹	M _w /M _n	% end-capping	f (= [D]/[H + D])	T _m /°C
2CFdPE5	5	7.1	1.05	84	0.43	96
PE50	50	56.6	1.04			106

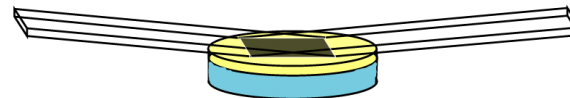
- Samples prepared by spin coating 1% polymer + additive in warm toluene at 2000 rpm onto silicon
- Resultant films ~1000Å thick

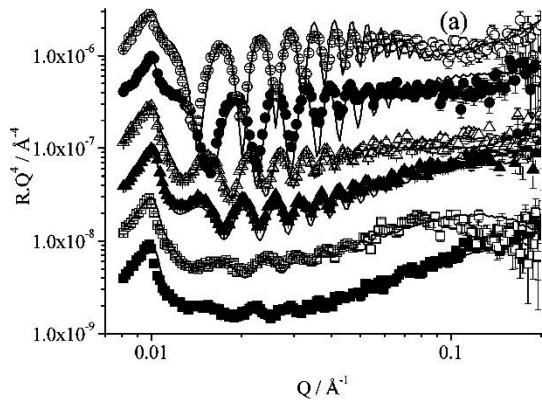


- XPS data confirm fluorocarbon present at film surface

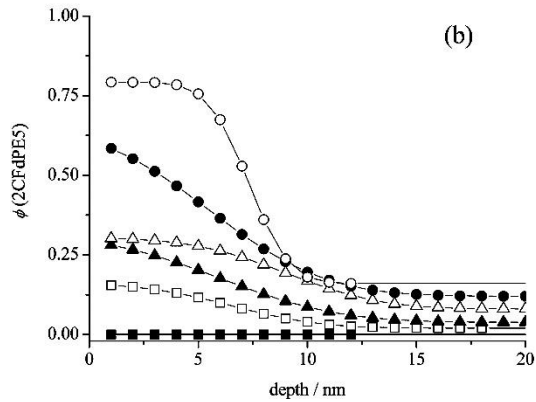


- NR on INTER at ISIS
- Samples heated to 120° C T_m~109°
- Data taken at 2 angles of incidence (0.6, 1.8°) with constant q resolution
- ~40 minutes per sample
- **Blended films neutron refractive index close to that of air**

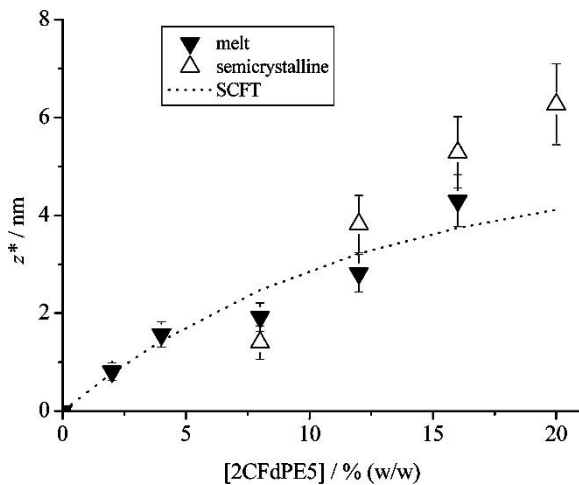




Kiessig fringes from film thickness: visibility proportional to additive surface excess



Data fitted to an error function profile
0,2,4,8,12,16% additive



Comparison of adsorbed amount determined by NR (melt), Nuclear Reaction Analysis and simulated by SCF theory ($\chi_b - \chi_s = 3.0k_B T$)



Conclusions

- Poly(ethylene) materials with well defined multi fluorocarbon functional groups produced
- As additives in blends generate films with enhanced hydrophobicity and lipophilicity
- At room temperature films are inherently crystalline but not sufficiently rough to give rise to super hydrophobicity (Wenzel wetting)
- Melting transition does not cause gross changes in self-organisation (NR Vs NRA data)



Acknowledgements

- Richard Thompson
- Sarah Hardman
- Lian Hutchings
- Nigel Clarke
- Solomon Kimani
- Laura Mears

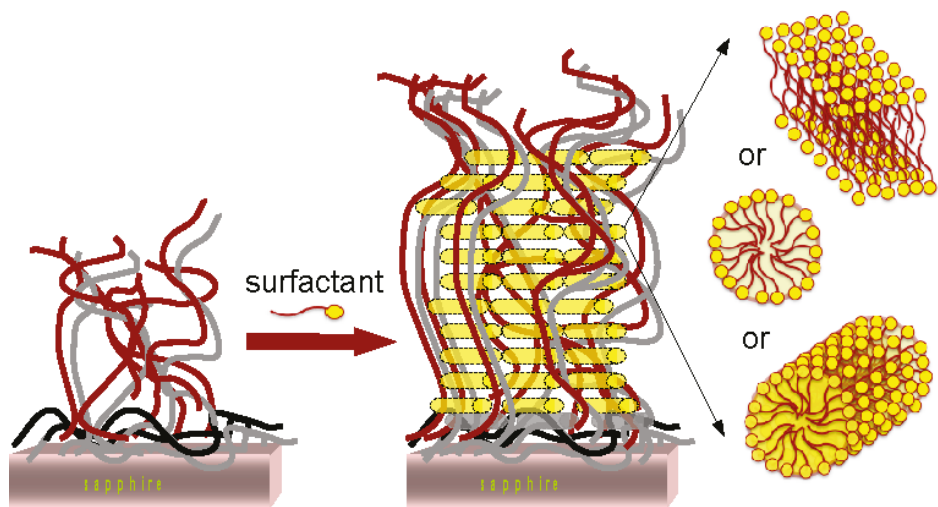
- Emily Smith

Durham (synthesis, NRA, Contact angle, AFM, SCF calculations)

Nottingham(XPS)

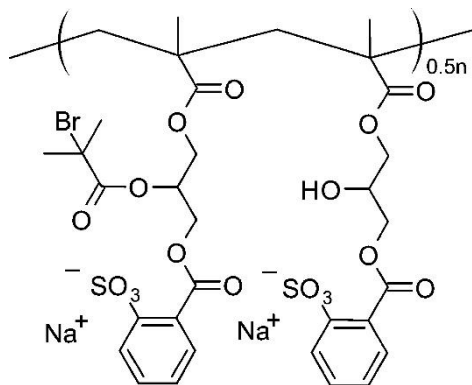


A Neutron Reflectivity Study of Surfactant Self-Assembly in Weak Polyelectrolyte Brushes at the Sapphire-Water Interface



- Poly(2-(dimethylamino)ethyl methacrylate) (PDMAEMA) Brushes and oppositely charged surfactant sodium dodecyl sulfate (SDS)
- PDMAEMA neutral at pH9 and cationic at pH3





- Polymer brushes grown by SI-ATRP onto sapphire substrate using a macroinitiator
- Characterised by ellipsometry, X-ray reflectivity, and neutron reflectivity measurements (Moglianetti et al. *Langmuir* 2010, 26, 12684–12689.)

sample	dry thickness (nm)	γ (Å)	Γ_{DMAEMA} (10^{-25} mol Å ⁻²)	σ (nm ⁻²)	N	M_w (kg/mol)
a	5	47	3.5 ± 0.3	0.13 ± 0.02	155	24 ± 5
b	11	100	7.4 ± 0.7	0.12 ± 0.02	443	70 ± 16
c	17	142	10.4 ± 1.0	0.14 ± 0.02	430	68 ± 15
d	17	167	12.4 ± 1.2	0.18 ± 0.03	434	68 ± 15



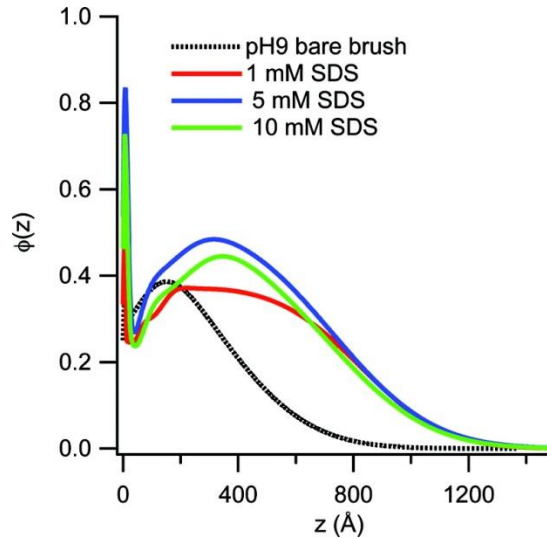
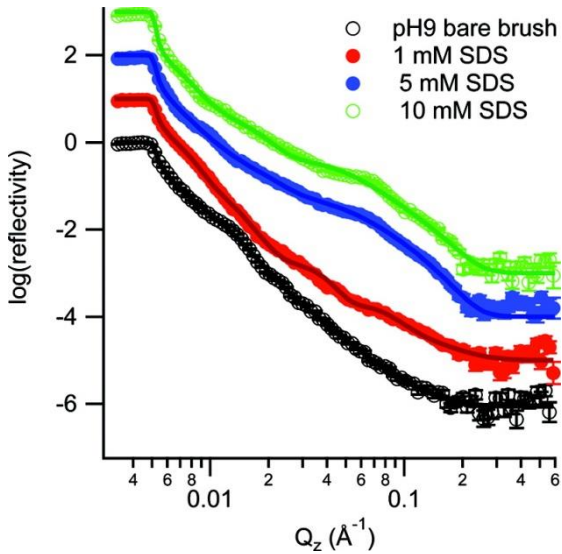
- NR data collected on the SURF reflectometer at ISIS
- Sapphire-D₂O qc $\sim 0.0048 \text{ \AA}^{-1}$
- 4 angles of incidence 0.1, 0.25, 0.7, 1.5° data combined to cover $0.0033 < q < 0.6 \text{ \AA}^{-1}$
- Reflectivity modelled as three to five layers each characterised by a thickness, scattering length density and Gaussian roughness.
- **SLD of segments and surfactant similar- determine VFP of SDS+DMAEMA**
- Polymer adsorbed amount known and constant (grafted, no free polymer)



$$\varphi(z) = \frac{\rho_{D_2O} - \rho(z)}{\rho_{D_2O} - \rho_{DMAEMA}}$$



pH 9 uncharged polymer (brush "d" dry thickness 17nm)



- No change in reflectivity up to 1 mM SDS
- Development of fringe corresponds to swelling of adsorbed layer

[SDS] (mM)

1

5

10

Γ_{SDS} (10^{-25} mol \AA^{-2})

4.6 ± 0.5

6.7 ± 0.7

5.3 ± 0.5

$n_{\text{SDS}}/n_{\text{DMAEMA}}$

0.37

0.55

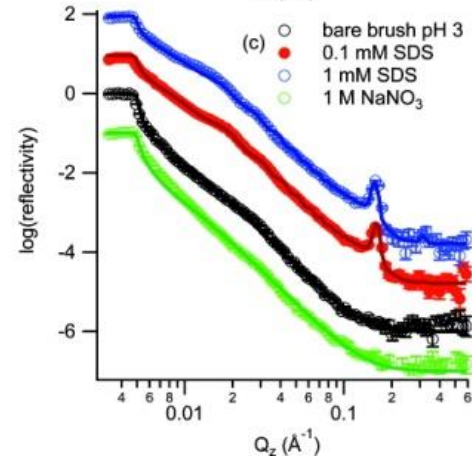
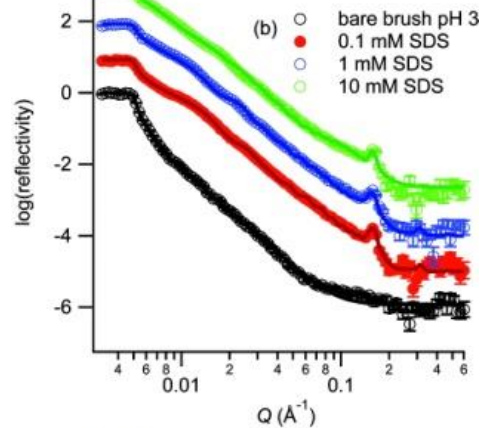
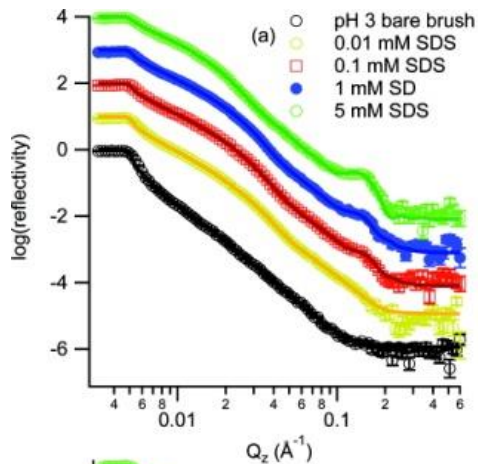
0.43

Onset of SDS adsorption analogous to CMC in bulk

Lowering of chemical potential in brush estimated from $c_{ac}/c_{mc} \sim 1.4k_B T$



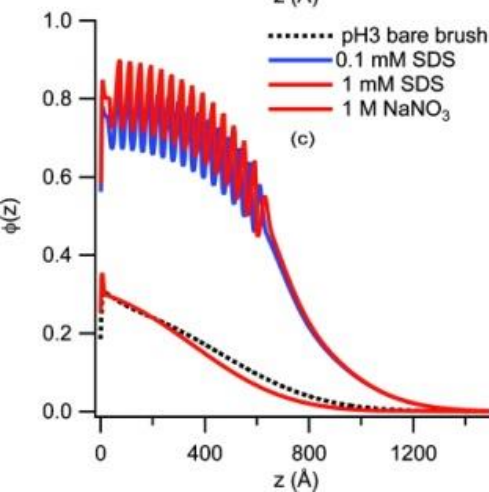
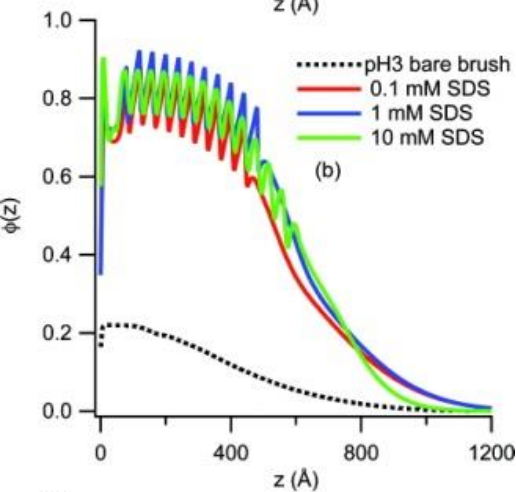
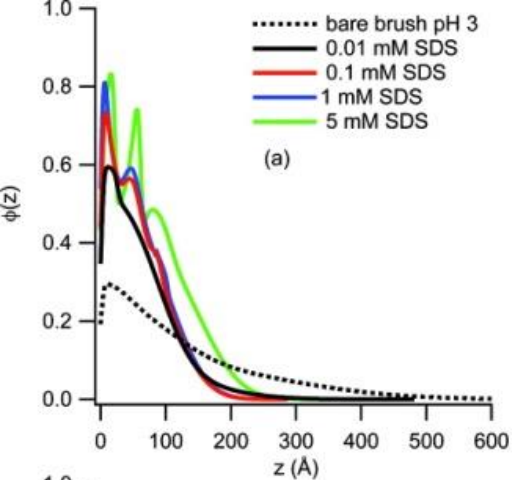
pH 3 cationic polymer



- Brushes a-c (5,11,17 nm dry brush) with increasing SDS concentration and with addition of salt
- No change in R when rinse with D2O
- Presence of Bragg peak indicates multilayers formed
- Addition of salt results in loss of Bragg peak
- As brush thickness increases onset of change in R at higher concentration (0.01 – 0.1 mM) with sharper Bragg peak
- Bragg peak position suggests spacing of $\sim 40 \text{\AA}$ typical of an SDS micelle or bilayer



Interfacial volume fraction profiles SDS+DMAEMA

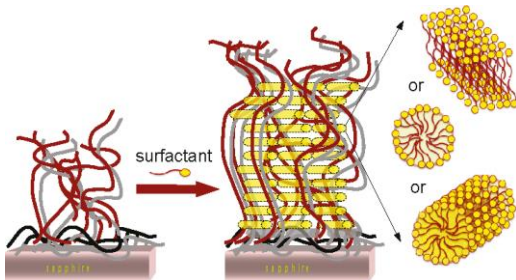


- 5nm brush 1-3 bilayers. Exchange of ions (OH^- , DS^-) $\sim 17.5\%$ at 0.01mM results in deswelling (loss of mobile counter-ions). Up to 0.35 SDS/DMAEMA
- 11nm brush 10-14 bilayers. Onset of uptake 0.1mM . Up to 2 SDS/DMEAMA. Excess DS^- over charged segments brings in Na^+ resulting in osmotic swelling
- 17nm brush 15 bilayers. Onset of uptake 0.1mM corresponding to $4.4 k_B T$ relative to SDS micelle. $\sim 3k_B T$ from screening of headgroup repulsions
- Addition of salt returns bare brush surface excess. Brush thickness $\sim 15\%$ less. Osmotic \rightarrow salted regime



Conclusions

- Polymer brushes provide a convenient method of systematically exploring the interactions between strongly interacting polyelectrolytes and surfactants
- PDMAEMA brushes of moderate grafting density exhibit significant uptake of the anionic surfactant SDS
- In the absence of PDMAEMA 89% of a single bilayer is formed at the sapphire-water interface at a SDS concentration of 7 mM
- At pH 3, multilayered surfactant aggregates form within the brushes, with a periodic repeat that is consistent with lamellae of SDS bilayers or a hexagonal phase of cylindrical SDS micelles
- At pH 9 electrostatic screening is absent but hydrophobic effect sufficient driving force for adsorption.



Acknowledgements

- Simon Titmuss Edinburgh
- Mauro Moglianetti EPFL
- Steve Armes Sheffield
- Steve Edmondson Loughborough

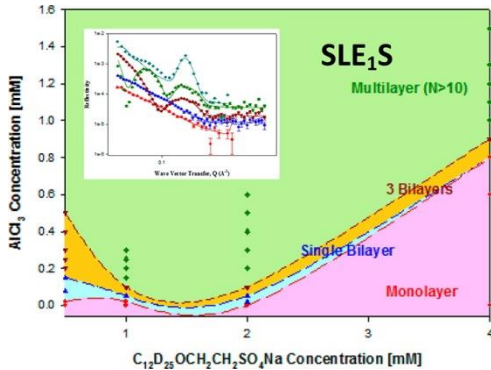




Surface Multilayers at the Air-Water Interface

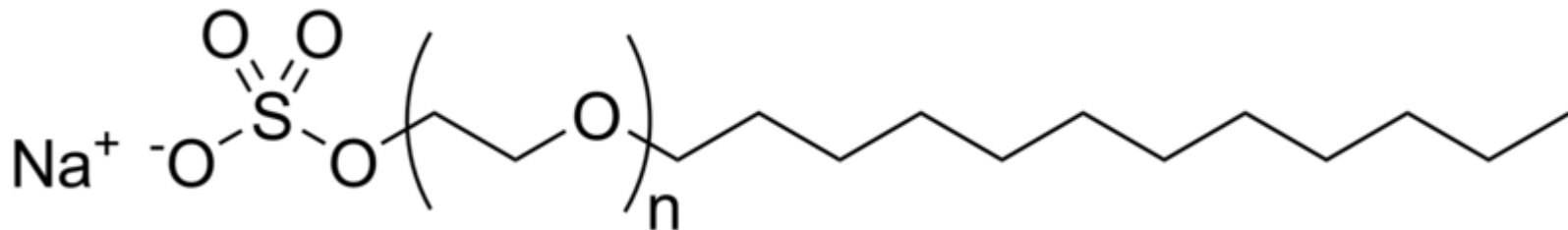


Surface Multilayers at the Air-Water Interface in Dilute Surfactant Solutions



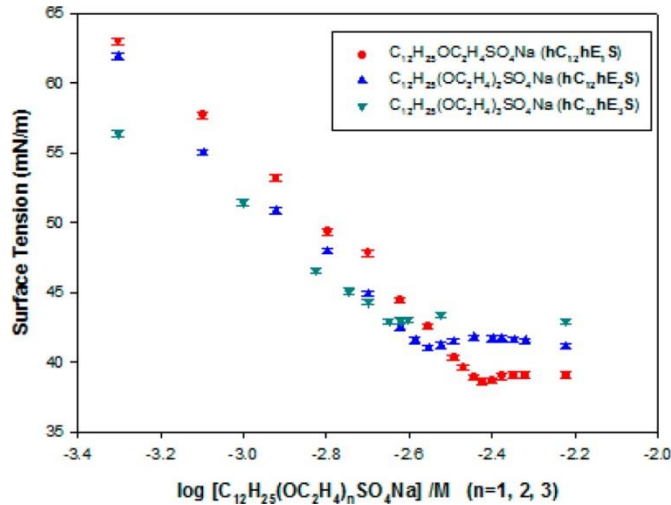
- sodium lauryl ether sulfate, SLES + Al^{3+}
- NR and ST used to study Surface Adsorption

Anionic detergent found in many personal care products (soaps, shampoos, toothpaste...) often in mixtures with non-ionics



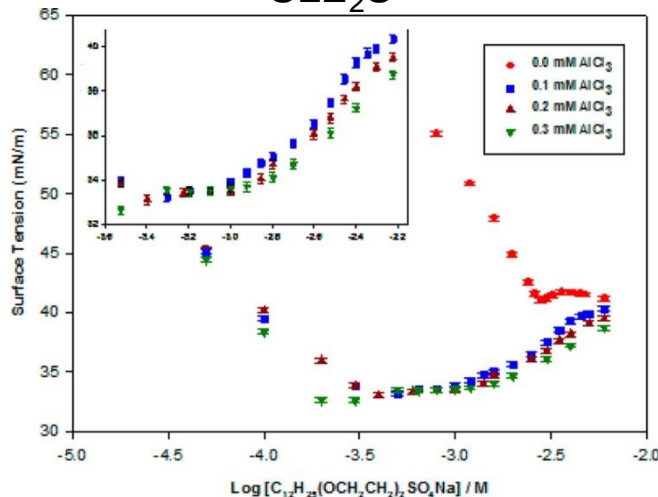


Surface Tension Without Al³⁺



- Small minimum -> low level of impurity, $\leq 0.01\%$.
- plateau region increases as eo length increases but CMC decreases
- ~greater tendency for micelle formation

SLE₂S



Surface Tension With Al³⁺

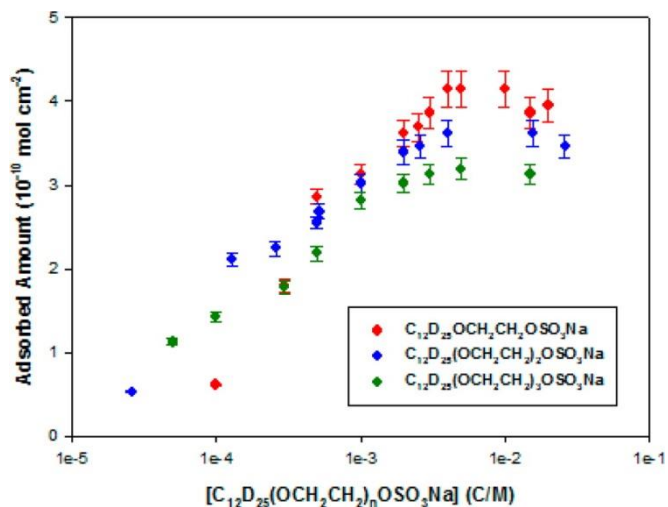
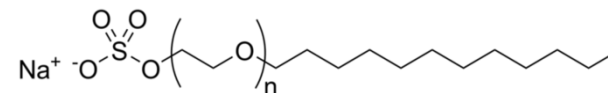
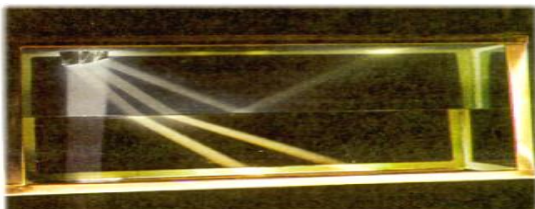
- Surface tension curve shifted to lower cmc in presence of Al³⁺
- As SLES in excess ST converges



NR Without Al³⁺

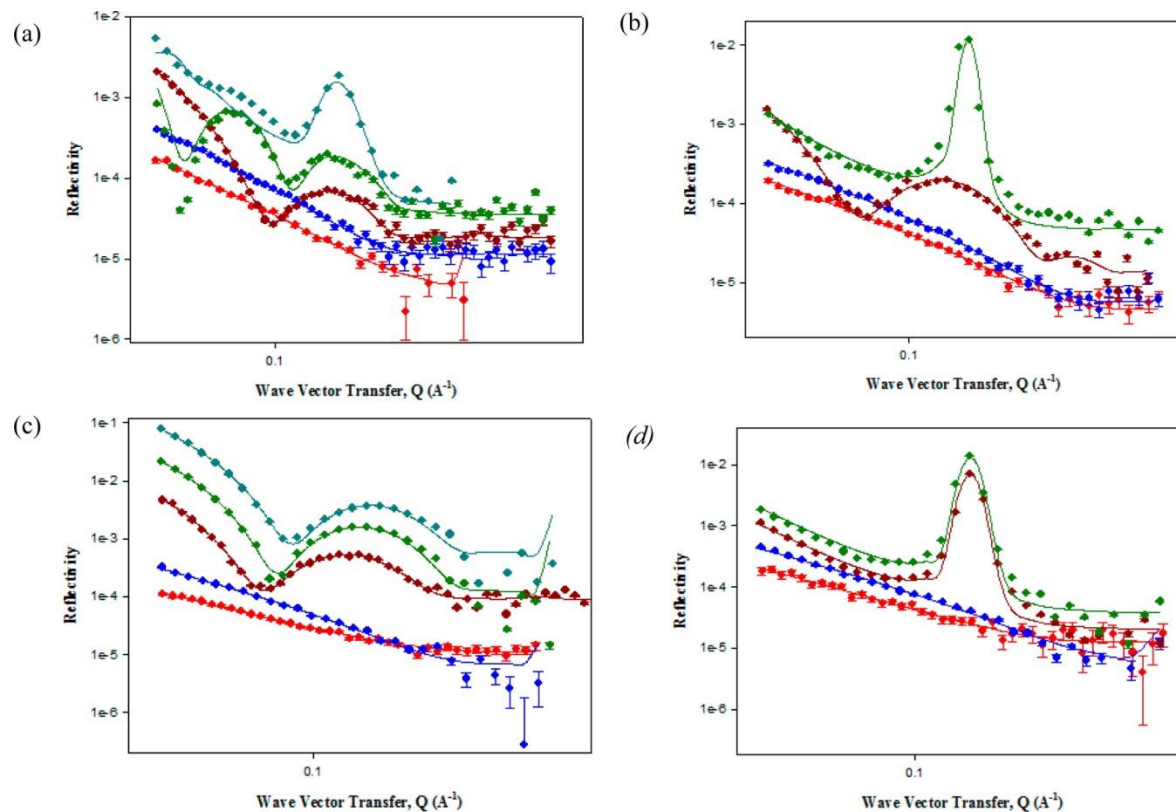
$$A = \sum b / d \cdot N_b$$

$$\Gamma = 1/A \cdot N_{av}$$



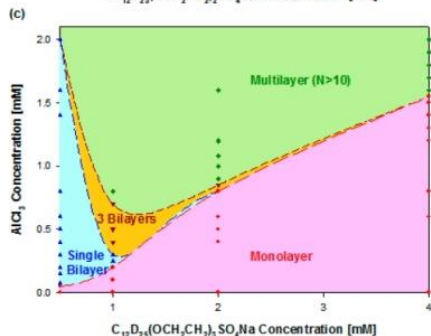
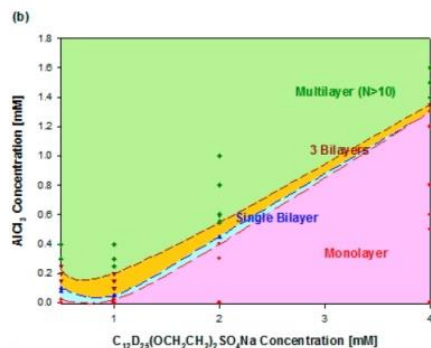
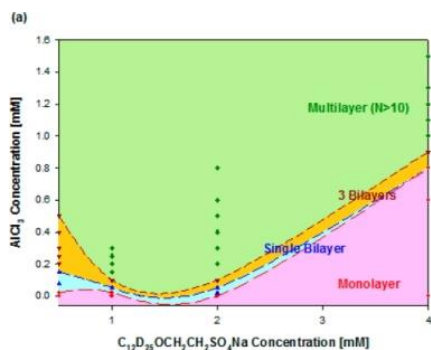
- alkyl chain d labelled SLES, dC12hE1S, dC12hE2S, and dC12hE3S.
- thin monolayer, $\sim 17 \pm 2$ Å, of uniform composition

NR With Al³⁺

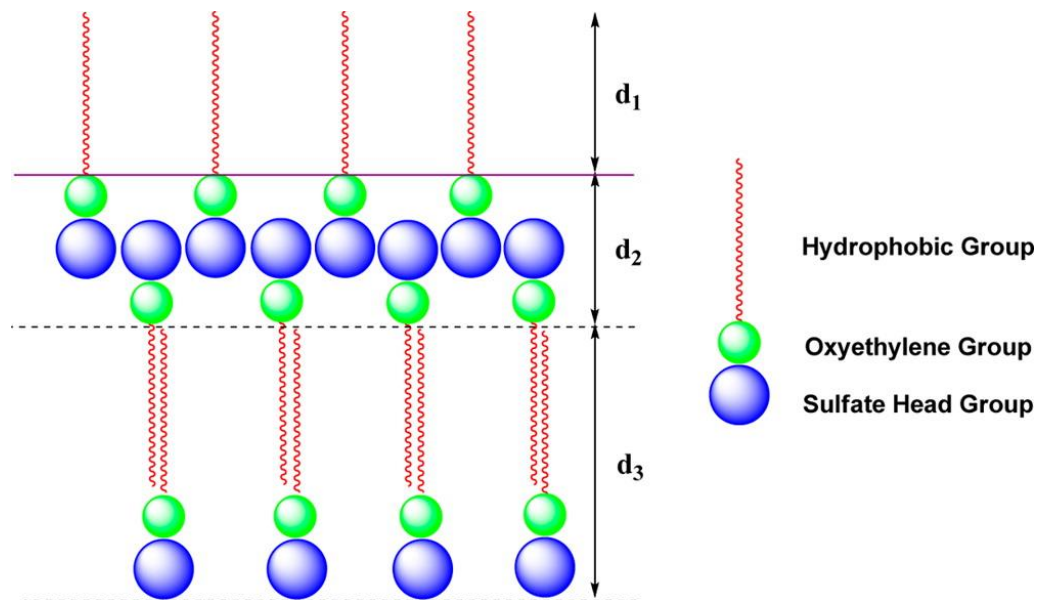


- (a) 1 mM SLE1S, 0.0 mM (red), 0.02 mM (blue), 0.05 mM (dark red), 0.1 mM (dark green), 0.2 mM AlCl₃ (dark cyan)
 (b) 2 mM SLE2S, 0.0 mM (red), 0.4 mM (blue), 0.5 mM (dark red), 0.6 mM AlCl₃ (dark green)
 (c) 0.5 mM SLE3S, 0.0 mM (red), 0.05 mM (blue), 0.15 mM (dark red), 0.5 mM AlCl₃ (dark green), 0.8 mM AlCl₃ (dark cyan)
 (d) 4 mM SLE3S, 0.0 mM (red), 1.5 mM (blue), 1.6 mM (dark red), and 1.8 mM AlCl₃ (dark green).

Approximate Surface Phase Diagrams For SLES / Al³⁺



- strong complexation between SLES and Al³⁺, transition from monolayer to surface multilayer structures
- EO1 – EO3 increase monolayer region - require more Al³⁺ to drive multilayers
- Increasing EO size disrupts complexation and multilayer formation



Reflectometry Summary

- Depth profile sensitive to number and type of atom
- $\sim 10\text{\AA}$ resolution
- Interface thickness $\sim 5\text{\AA}$ to 5000\AA
- 'buried' interfaces
- Contrast variation
 - invisible substrate
 - Pick out components in complex mixtures
 - unique structure determination

Background material

The following review articles, book chapter, and book provide a useful background to Neutron Reflectivity. The articles and book chapter are readily available on line and the book is available from most on-line outlets, such as Amazon.

(a) Basic Reviews on Neutron and x-ray reflectivity

- (1) J Penfold, RK Thomas, J Phys: Condens Matt 2 (1990) 1369
- (2) TP Russell, Mat Sci Rep 5 (1990) 171

(b) Applications of neutron reflectivity in surfactants and polymer-surfactant

- (1) JR Lu, RK Thomas, J Penfold, Adv Coll Int Sci 84 (2000) 143
- (2) DJF Taylor, RK Thomas, J Penfold, Adv Coll Int Sci 132 (2007) 69
- (3) J Penfold, RK Thomas, Int Sci and Technol, Adv Chem of Monolayers and Interfaces, Vol 14, Chapt 4, 87-115, Ed I Imae, Elsevier, 2007.

(c) Basic scattering theory

- (1) Elementary Scattering Theory for x-ray and neutron users, DS Sivia, OUP, 2011, ISBN 978-0-19-922868-3